

Spatiotemporal Dynamics of Vision on Force Control

BY

CYNTHIA POON

B.S., University of Illinois at Chicago, Chicago, IL, 2007

M.S., University of Illinois at Chicago, Chicago, IL, 2009

THESIS

Submitted as partial fulfillment of the requirements
for the degree of Doctor of Philosophy in Movement Sciences
in the Graduate College of the
University of Illinois at Chicago, 2012

Chicago, Illinois

Defense Committee:

Daniel Corcos, Chair and Advisor
David Vaillancourt, Advisor, University of Florida
Janey Prodoehl
Stewart Shankman, Psychology
Stephen Coombes, University of Florida

This thesis is dedicated to my mom, dad, sisters, and brother.

ACKNOWLEDGEMENTS

I would like to thank the members of my dissertation committee, Drs. David Vaillancourt, Daniel Corcos, Stephen Coombes, Janey Prodoehl, and Stewart Shankman for their time and commitment during the completion of this thesis. Dr. Vaillancourt, I cannot thank you enough for the dedication and support that you have provided as my advisor throughout my doctoral education. Dr. Corcos, I cannot thank you enough for being a wonderful master's and doctoral advisor over the past five years. I really appreciate all the time and energy that both of you have taken into shaping me to be a better scientist. And thank you both for being the most caring, devoted, and inspiring mentors that I can ever ask for. I would like to thank Dr. Coombes and Dr. Prodoehl for their valuable advice and support while working on various projects at the lab. I would like to thank Dr. Shankman for taking the time out of his busy schedule to serve on my committee and providing valuable feedback on the topic of EEG.

Next, I would like to thank all of the past and present members of the Motor Control and Movement Disorders Group, especially Dr. Fabian David, Mrs. Lisa Chin-Cottongim, Dr. Julie Robichaud, and Dr. Mark Shapiro, for their friendship, guidance, and support throughout my many memorable years at the lab. Without all of you, I would not have been able to finish my dissertation. I am definitely one of the luckiest person in the world to have worked in a lab with the smartest and nicest people I know. These years have been a joy with all of your company!

Lastly, I would like to thank my family and friends who have provided a great network of support and encouragement throughout this process. I would like to especially thank my parents for raising me to be who I am today and providing me the opportunity to pursue “happiness”. (謝謝你 媽媽和爸爸) I would like to thank my sister, Rachel, and my boyfriend, Will, for

helping me stay focused (most of the time) and being understanding throughout my academic pursuit.

TABLE OF CONTENTS

CHAPTER 1

1. INTRODUCTION

1.1 Organization of the Dissertation.....	1
1.2 Visually guided and internally guided movements.....	1
1.3 Effects of visual gain on force and motor control.....	3
1.4 Event-related Electroencephalography (EEG).....	5

CHAPTER 2

2. SPATIOTEMPORAL DYNAMICS OF BRAIN ACTIVITY DURING THE TRANSITION FROM VISUALLY GUIDED TO MEMORY GUIDED FORCE CONTROL

2.1 Introduction.....	11
2.2 Research Design and Methods.....	13
2.2.1 Subjects.....	13
2.2.2 Experimental design.....	14
2.3 Data Acquisition and Statistical Analysis.....	17
2.3.1 Behavioral data acquisition.....	17
2.3.2 Electrophysiological data acquisition.....	17
2.3.3 Behavioral data analysis.....	18
2.3.4 Electrophysiological data analysis.....	20
2.3.5. Source estimation analysis.....	22
2.4 Results.....	23
2.4.1 Behavioral results.....	23
2.4.2 Electrophysiological results.....	25
2.4.3 Source estimation results.....	27
2.5 Discussion.....	32
2.5.1 Premotor activation.....	32
2.5.2 Prefrontal activation.....	33
2.5.3 Frontal-parietal network of motor memory.....	34
2.5.4 Summary.....	35

CHAPTER 3

3. SPATIOTEMPORAL DYNAMICS OF BRAIN ACTIVITY DURING ADAPTATION TO CHANGES IN VISUAL GAIN

3.1 Introduction.....	37
3.2 Research Design and Methods.....	39
3.2.1 Subjects.....	39
3.2.2 Experimental design.....	40
3.3 Data Acquisition and Statistical Analysis.....	45
3.3.1 Behavioral data acquisition.....	45

TABLE OF CONTENTS (continued)

3.3.2 Electrophysiological data acquisition.....	46
3.3.3 Behavioral data analysis.....	48
3.3.4 Electrophysiological data analysis.....	48
3.3.5 Correlation analysis.....	51
3.3.6 Source estimation analysis.....	52
3.4 Results.....	52
3.4.1 Low to high visual gain: Behavioral results.....	52
3.4.2 High to low visual gain: Behavioral results.....	53
3.4.3 Low to high visual gain: Electrophysiological results.....	56
3.4.4 High to low visual gain: Electrophysiological results.....	60
3.4.5 Behavioral and electrophysiological correlation.....	61
3.4.6 Experiment 2: Source estimation results.....	61
3.5 Discussion.....	70
3.5.1 Behavioral correlation to event-related cortical activity.....	70
3.5.2 Regions involved with immediate increases in visual gain.....	72
3.5.3 Regions involved with immediate decreases in visual gain.....	73
3.5.4 Common regions involved with immediate changes in visual gain.....	73
3.5.5 Summary.....	74

CHAPTER 4

4. CONCLUSIONS

4.1 Chapter 2 conclusions.....	76
4.2 Chapter 3 conclusions.....	77

CITED LITERATURE.....79

APPENDIX.....86

VITA.....90

LIST OF TABLES

<u>Table</u>	<u>Page</u>
2.1. Statistical results for memory guided force control.....	29
3.1. Statistical results for low-high visual gain transition.....	59
3.2. Statistical results for high-low visual gain transition.....	68
3.3. Coordinates of maximum activation as revealed by LORETA.....	69

LIST OF FIGURES

<u>Figure</u>	<u>Page</u>
2.1. A: precision grip apparatus pressed with the subject's thumb and index fingers. B: sequence of conditions for each trial along with the visual display viewed by the subject. The transition periods are identified in vertical dashed lines.....	15
2.2. Clusters of 3 electrodes (<i>gray-filled circles</i>) are highlighted with dashed lines showing the 13 regions of interest (ROIs). Black-filled circles are the two reference electrodes used during data collection.....	19
2.3. The eight 100ms time bins used to compare between fixation and memory transitions.....	21
2.4. A: Subject's mean force output before and after visual feedback was removed. B: Standard deviation (SD) and C: Coefficient of variation (CV) of force. D: Root mean squared error (RMSE) of force production relative to the target force following the removal of visual feedback.....	24
2.5. Grand-average event-related topography in 100 ms time bins from -200 ms to 800 ms after (A) fixation transition and (B) memory transition.....	26
2.6. Grand-average event-related potentials (ERPs) of regions of interest (ROIs) in the memory transition (<i>black</i>) and fixation transition (<i>gray</i>). Statistically significant ROIs are highlighted chronologically from earliest to latest time of significance (i.e. <i>green</i> to <i>yellow</i> to <i>red</i>). * indicates significant time bins within each ROI.....	30
2.7. Grand-averaged ERP difference results of the LORETA analysis showing current density maxima from 300-400 ms (top row), 400-500 ms (middle row), and 500-600 ms time bins (bottom row). Each map consists of axial, coronal, and sagittal slices showing the same area of maximum activation.....	31
3.1. A: precision grip apparatus pressed with the subject's thumb and index fingers. B: sequence of conditions for each trial along with the visual display viewed by the subject. The transition periods are identified in vertical dashed lines.....	41
3.2. The calculation for visual angle was determined by the distance from the eye to the monitor, along with the height of the force fluctuations viewed on the computer monitor.....	43

LIST OF FIGURES (continued)

<u>Figure</u>	<u>Page</u>
3.3. Clusters of 3 electrodes (<i>gray-filled circles</i>) are highlighted with dashed lines showing the 13 regions of interest (ROIs). Black-filled circles are the two reference electrodes used during data collection.....	47
3.4. The eight 100ms time bins used to compare between fixation and gain transitions in Experiment 1 and Experiment 2.....	50
3.5. Experiment 1 behavioral data. A: Subject’s mean force output before and after low to high gain transition. B: Standard deviation (SD) and C: Coefficient of variation (CV) of force. C: Root mean squared error (RMSE) of force production relative to the target force following low to high gain change.....	54
3.6. Experiment 2 behavioral data. A: Subject’s mean force output before and after high to low gain transition. B: Standard deviation (SD) and C: Coefficient of variation (CV) of force. C: Root mean squared error (RMSE) of force production relative to the target force following high to low gain change.....	55
3.7. Experiment 1: Grand-average event-related topography in 100 ms time bins from -200 ms to 800 ms after (A) fixation transition and (B) low-high gain transition. The potential distribution is projected onto a standardized head shape.....	57
3.8. Experiment 1: Grand-average event-related potentials (ERPs) of regions of interest (ROIs) in the low-high gain transition (<i>black</i>) and fixation transition (<i>gray</i>). Statistically significant ROIs are highlighted chronologically from earliest to latest time of significance (i.e. <i>green</i> to <i>yellow</i>). * indicates significant time bins within each ROI.....	58
3.9. Experiment 2: Grand-average event-related topography in 100 ms time bins from -200 ms to 800 ms after (A) fixation transition and (B) high-low gain transition. The potential distribution is projected onto a standardized head shape.....	63
3.10. Experiment 2: Grand-average event-related potentials (ERPs) of regions of interest (ROIs) in the high-low gain transition (<i>black</i>) and fixation transition (<i>gray</i>). Statistically significant ROIs are highlighted chronologically from earliest to latest time of significance (i.e. <i>green</i> to <i>yellow to red</i>). * indicates significant time bins within each ROI.....	64

LIST OF FIGURES (continued)

<u>Figure</u>	<u>Page</u>
3.11. Force variability (SD) and event-related brain activity of significant ROIs in Experiment 1 (A) and Experiment 2 (B). Each data point represent the grand average voltage change across subjects to the force variability at each 100 ms time bin from -200 to 800 ms after force transition. The lines are the linear regression lines.....	65
3.12. Experiment 1: Grand-averaged ERP difference results of the LORETA analysis showing current density maxima from 300 to 400 ms (top row), 400 to 500 ms (top middle row), 500 to 600 ms (bottom middle row), and 600 to 700 ms time bins (bottom row). Each map consists of axial, coronal, and sagittal slices showing the areas of maximum activation.....	66
3.13. Experiment 2: Grand-averaged ERP difference results of the LORETA analysis showing current density maxima from 300 to 400 ms (top row), 400 to 500 ms (top middle row), 600 to 700 ms (bottom middle row), and 700 to 800 ms time bins (bottom row). Each map consists of axial, coronal, and sagittal slices showing the areas of maximum activation.....	67

LIST OF ABBREVIATIONS

ACC	Anterior cingulate cortex
AIP	Anterior intraparietal sulcus
ANOVA	Analysis of variance
AP	Action potential
APEN	Approximate entropy
BOLD	Blood oxygenation level dependent
CMS	Common mode sense
CV	Coefficient of variation
DLPFC	Dorsolateral prefrontal cortex
DRL	Driven right leg
EEG	Electroencephalography
ERD	Event-related desynchronization
ERN	Error-related negativity
ERP	Event-related potential
ERS	Event-related synchronization
fMRI	Functional magnetic resonance imaging
GABA	γ -aminobutyric acid
HSD	Honestly significant difference
IPL	Inferior parietal lobule
IPS	Intraparietal sulcus
LIP	Lateral intraparietal sulcus
LGN	Lateral geniculus nucleus

LIST OF ABBREVIATIONS (continued)

LORETA	Low-resolution electromagnetic tomography
M1	Primary motor cortex
MEG	Magnetoencephalography
MIP	Medial intraparietal sulcus
MTL	Medial temporal lobe
MVC	Maximum voluntary contraction
Pe	Error-related positivity
PET	Positron emission tomography
PMd	Dorsal premotor cortex
PMv	Ventral premotor cortex
PPC	Posterior parietal cortex
PSP	Postsynaptic potential
ROI	Region of interest
RMSE	Root-mean-squared error
SD	Standard deviation
SMA	Supplementary motor area
SPL	Superior parietal lobule
TFA	Time-frequency analysis
TMS	Transcranial magnetic stimulation
uV	Microvolts
V	Volts
WM	Working memory

SUMMARY

Most human behavior involves using visual information to complete everyday tasks such as reaching for objects and driving a car. Seminal studies have emphasized the detrimental effects of movements without visual guidance (Carlton 1981; Keele and Posner 1968; Woodworth 1899). In addition, varying spatial and temporal features of visual information have been shown to influence motor performance (Coombes et al. 2010b; Slifkin et al. 2000; Vaillancourt et al. 2006a). Spatiotemporal features of visual feedback can be manipulated by altering the frequency, distance, or amplitude at which visual feedback is presented. Visual information is especially important during continuous force and motor control because of the temporal capacity of our visuomotor system (Slifkin et al. 2000; Vaillancourt and Russell 2002). A model of visuomotor control has been proposed where visual information may be processed at a much faster rate (~6.4Hz) than our motor system can execute a response (~1-2Hz) (Slifkin et al. 2000, Miall et al. 1996). This emphasizes the importance of temporal dynamics in regulating visual information and maintaining accurate force control. Much is now known about the brain regions of our visuomotor system and how they are affected with varying visual manipulations (Coombes et al. 2010b), but less is understood about the immediate response of the visuomotor system to changing spatiotemporal features of visual feedback. Hence, this dissertation explores the dynamic spatiotemporal pattern of brain activity during precision grip force in healthy individuals. This dissertation will allow us to gain fundamental insights into human visuomotor control through a technique that enables us to record at a high temporal resolution.

The first study of this dissertation examined the spatiotemporal pattern of brain activity during the immediate transition from a visually guided to a memory guided force control task using event-related potentials (ERPs) and low-resolution electromagnetic tomography (LORETA

SUMMARY (continued)

) on grand-averaged ERP differences. We measured 128-channel scalp electroencephalography (EEG) on twelve healthy young adults while they performed an isometric precision grip force task. A significant change in EEG activity was detected in the ERPs and source localization confirmed the observed ERP findings. Our findings show that subjects rely on sensorimotor memory processes involving left ventral premotor cortex and right ventral prefrontal cortex after the immediate transition from visually guided to memory guided force control.

The second study examined the spatiotemporal pattern of brain activity during the immediate transition between different spatial amplitudes of visual feedback using event-related potentials (ERPs) and low-resolution electromagnetic tomography (LORETA) on grand-averaged ERP differences. The transition consisted of going from a low to high visual gain (Experiment 1) and high to low visual gain (Experiment 2). We measured 128-channel scalp EEG on healthy individuals while they performed two isometric precision grip force tasks. Increasing visual gain (Experiment 1) involves a shift in electrocortical activity within parietal-frontal circuits that is not present during decreases in visual gain. More importantly, the parietal-frontal brain activity systematically relates to force error during increases in visual gain. The transition from low to high visual gain involves greater changes in the superior parietal cortex, while the transition from high to low visual gain involves greater changes in occipital regions such as the right extrastriate cortex (V3). Activity in the dorsal and ventral premotor cortices was identified during both low to high and high to low changes in visual gain. Our results suggest that increased visual gain triggered increased force variability that was related to electrocortical activity in parietal-frontal circuits.

CHAPTER 1

INTRODUCTION

1.1. Organization of the dissertation

The overall purpose of this dissertation is to examine the spatiotemporal pattern of brain activity during force control in healthy individuals using high-density electroencephalography (EEG). Chapter 1 reviews previous work that has identified how visually guided and internally guided tasks are controlled by a widespread network of cortical and subcortical brain areas. Then, I will be reviewing the literature on how visual gain influences force and motor control. Lastly, I will be providing an overview on the basic principles of event-related electroencephalography (EEG). Chapter 2 investigates brain activity during the transition from a visually guided to memory guided force control task. Chapter 3 investigates brain activity during adaptation to visual gain changes, specifically the immediate transition from low to high visual gain levels and high to low visual gain levels. All experiments examined the spatiotemporal dynamics of brain activity using event-related potentials (ERPs) and low-resolution electromagnetic tomography (LORETA) of grand-averaged ERP differences. Lastly, Chapter 4 summarizes the findings of this dissertation.

1.2. Visually guided and internally guided movements

The use of visual information in the control of movement involves a complex network of brain regions. Visual areas of the brain must be connected to motor areas for the correct guidance of movements. As vision enters our eyes and projects onto our retina, the information travels down the optic tract to project to several areas including the hypothalamus and lateral geniculate nucleus (LGN). The information from the LGN then goes on to project onto the primary visual

cortex (V1/striate cortex). Within layers 4 of the striate cortex is where information from the two eyes converge. Next, the visuomotor pathway is classically viewed as separating into two pathways identified as the dorsal and ventral streams of visual cortex (Mishkin et al. 1982). The dorsal stream, commonly known as the “where” pathway, projects information about the spatial location and orientation of objects in space. The ventral stream, commonly known as the “what” pathway, is primarily responsible for object recognition and identification of object properties. Both V1 and V2 project via the dorsal pathway to the middle temporal area (MT/V5), which then projects to the posterior parietal cortex (PPC). The dorsal pathway plays a crucial role during visually guided movements with motion and spatial awareness. Many studies have discussed the role of regions involved with this pathway during visually guided movements. Damage to the parietal cortex has been shown to cause disturbances during visually guided movements (Caminiti et al. 1996; Grea et al. 2002). A number of regions within the parietal cortex, around the intraparietal sulcus (IPS), have been linked with visuomotor control such as the medial intraparietal sulcus (MIP) during reaching, lateral intraparietal sulcus (LIP) during eye movements and saccades, and anterior intraparietal sulcus (AIP) during grasping (Caminiti et al. 1996; Culham et al. 2006; Jeannerod et al. 1995). Subsequent evidence for the transfer of visual information from the parietal cortex to the motor cortex has been shown through direct cortical recording of neurons within the motor and parietal regions of non-human primates (Caminiti et al. 1991; Jeannerod et al. 1995; Johnson et al. 1996). In addition to the premotor and parietal cortex, the cerebellum and basal ganglia have also been shown to be involved during visually guided movements (Glickstein 2000; Miall et al. 2001; Middleton and Strick 1998; Prodoehl et al. 2009; Vaillancourt et al. 2003). Because the cytoarchitecture of subcortical regions are composed largely of unaligned cells and located deeper within the brain, it is unlikely

that EEG is able to detect these potentials at the scalp surface. Therefore the focus of this dissertation will be on cortical structures only.

In the absence of visual information, a different network of brain regions is commonly thought to be involved during movement. Neurophysiological evidence in non-human primates have suggested a functional division of the premotor cortex, specifically the lateral premotor cortex and supplementary motor area (SMA), to visually- and internally-guided movements, respectively (Mushiake et al. 1991; Passingham 1993). Anterior cerebellar (Debaere et al. 2003; Kawashima et al. 2000) and basal ganglia (Vaillancourt et al. 2003) functions have also been linked to internally-generated movements. Studies that examined internally-guided movements have been linked to a prefrontal-frontal-parietal circuit involving the supplementary motor areas, cingulate cortex, and inferior parietal cortex during movements (Debaere et al. 2003; Jahanshahi et al. 1995; Mueller et al. 2007) and the dorsolateral prefrontal cortex (DLPFC), ventral prefrontal cortex, and anterior cingulate cortex (ACC) during isometric force control (Vaillancourt et al. 2003). These findings suggest that a distributed network extends to prefrontal memory circuits during internally guided movements.

1.3. Effects of visual gain on force and motor control

When humans perform visually guided movements, the spatial qualities of visual feedback affect the motor response to a task. These spatial qualities could be manipulated by changes in visual gain, which is the sensitivity of a system to error. A common approach used to study sensorimotor processes in humans is to alter the gain of visual feedback. It has been well established that populations of neurons within the nonhuman primary visual cortex could be tuned to spatiotemporal properties of visual stimuli (Priebe et al. 2006; Rosenbluth and Allman

2002). Many studies have shown that amplifying the gain of visual feedback will improve performance during force (Newell and McDonald 1994b; Vaillancourt et al. 2006a) and movement control (Beuter et al. 1995; Prager and Contreras-Vidal 2003; Seidler et al. 2001b). More specifically, higher levels of visual gain have been shown to reduce the magnitude (standard deviation, SD and coefficient of variation, CV) and regularity (approximate entropy, ApEn) of force variability (Hong and Newell 2008; Sosnoff and Newell 2006). However, an inverted-U relationship between visual gain and motor performance has been shown where increasing gain will continue to improve performance up until a certain point, then continued increase in gain will lead to performance deficits (Beuter et al. 1995; Sosnoff and Newell 2006). Several studies have demonstrated large changes in force error with visual gain levels of less than 1° (Hong and Newell 2008; Vaillancourt et al. 2006a). Increases in visual gain up to 1° led to large improvement in force performance and small changes in the spatial amplitude of visual feedback. Increases in visual gain greater than 1° led to small changes in force performance but large changes in the spatial amplitude of visual feedback.

Accurate performance in visually guided movements depend on a visuomotor system consisting of specific regions in the parietal cortex, premotor cortex, SMA, basal ganglia, and cerebellum (Krakauer et al. 2004a; Roitman et al. 2009; Vaillancourt et al. 2003). The lateral cerebellum (Vaillancourt et al. 2006b) and putamen (Turner et al. 2003) have been positively associated with changes in visual feedback. Specific regions of the visuomotor system were also shown to respond selectively to changes in visual gain. Coombes and colleagues (2010a) found that large changes in force error and small changes in spatial amplitude were associated with increases in activation in V3 and V5 of the extrastriate visual cortex, primary motor cortex (M1), and ventral premotor cortex (PMv). On the other hand, small changes in force error and large

changes in spatial amplitude were associated with increases in activation in the dorsal and ventral premotor areas (PMd/PMv) and inferior parietal lobule (IPL). Another recent study by Coombes and colleagues (2010b) manipulated both the gain and frequency of visual feedback and found that the frequency of visual feedback drives where in the brain visual gain mediated improvements in force performance are regulated. Increasing visual gain at a high frequency led to increased activity in classic visuomotor areas including M1, SMA, PMv, SPL, IPL, and V5. Increasing visual gain at a low frequency led to increased activity in M1, PMd, IPL, SMA, and areas of the frontal-striatal circuit including DLPFC, ACC, caudate, and putamen. These findings suggest that increasing visual gain at different frequencies utilizes different circuits of the visuomotor system, with lower frequency requiring additional frontal-striatal regions to regulate motor performance.

1.4. Event-related Electroencephalography

Surface electroencephalography (EEG) is the recording of electrical activity along the scalp of an individual's head. The first ever recording on humans was performed by Hans Berger in 1924. He termed the recording "electroencephalography" and later showed that direct cortical recording of the brain is very similar to EEG recording with the exception of the signal being substantially smaller in amplitude during EEG recording. The electrical signal is recorded as a voltage difference in relation to a reference chosen by the experimenter. Two of the most common types of references used are the linked-ear reference and common average reference (Cacioppo et al. 2000).

The post-synaptic local field potentials (PSP) of pyramidal neurons within the cortex are thought to produce the majority of EEG signals. Action potentials (APs) are first generated

when a neuron's threshold is reached and Na^+ ions travel across the axon to the axon terminal. This inward current flow triggers a reciprocal outward current flow of K^+ ions in order to return the membrane back to its original resting state. This inward current results in a current sink and the outward current results in a current source that together form a dipole. Once the AP reaches the axon terminal, positive Ca^{++} ions are released which then triggers the release of neurotransmitter onto the receptors of dendrites. This results in the opening of ion channels and generation of PSP at the post-synaptic membrane. There are two types of PSPs, excitatory PSPs (EPSPs) and inhibitory PSPs (IPSPs). EPSPs are due to the depolarization of cell membrane which results in the opening of positive ion channels, an influx of positive ions, and the formation of a negative local field potential in the extracellular space. IPSPs are due to the hyperpolarization of membrane which results in a positive local field potential. About 90% of our neurons are of the EPSP-type. The most common neurotransmitter associated with EPSP is glutamate and the most common neurotransmitter for IPSP is GABA. EPSP favors superficial layers of the cortex while IPSP favors deeper layers of the cortex (Holmes and Khazipov 2007).

The action potentials (APs) were once thought to be a source of the EEG signals but were later proven to be highly unlikely. It is the different spatial and temporal features of APs and PSPs that led to the consensus that EEG signals are predominantly from PSPs. First, APs are generated at a higher frequency (one ms) than PSPs (tens or hundreds of ms), so there is a greater likelihood of APs to be filtered out by the high filtering properties of the human head (i.e. volume conduction of the scalp, skull, meninges, cerebral spinal fluid and other biological tissues) (Luck 2005). PSPs, on the other hand, are slower, graded potentials which allows for the summation of local field potentials from adjacent neurons. Secondly, the currents from graded potentials (PSPs) travel through cells and exit at relatively distant areas while APs are a series of

current sinks and sources located close together making it highly likely for local field potentials to cancel one another. Lastly, the spatial configuration of dendrites versus axons on pyramidal neurons makes PSPs a more likely source of EEG signals than APs. Dendrites are predominantly arranged in parallel to one another, tangential to the scalp, which creates a better configuration (also known as “open field” assembly) for the summation of PSPs. Axons are more likely to be arranged in a random fashion (“closed field”) so their polarities will likely cancel each other out (Cacioppo et al. 2000 and Holmes and Khazipov 2007). In summary, scalp-recorded EEG are thought to originate from post-synaptic potentials due to specific spatial and temporal features, 1) the slower graded potentials at the post-synaptic membrane, 2) the currents of graded potentials traveling and exiting at relatively distant areas, and 3) the parallel alignment of open field neuronal assemblies all allow for the summation of local field potentials.

To measure brain activity that is a direct result of cognitive processes like perception and memory, a series of EEG signals could be averaged together relative to a time-locked stimulus or event, also known as event-related potentials (ERPs) (Dawson 1947; Vaughan 1969). An ERP is formed from the summation of a series of EEG recordings, time-locked and phase-locked to a specific event or stimulus. George Dawson (1947) believed that by superimposing a series of 50 trials during electrical stimulation of the peripheral nerve, he would be able to pick up signals that are distinct and separate from the “noisy” background activity of EEG. He was able to detect deflections, contralateral to side of stimulation, starting as early as 22ms after stimulation. He concluded that the deflections were not due to electrical interference (as no such deflections were observed in control trials with no stimulation), muscular artifact (as the strongest deflections were found along the midline of scalp), or reflexes. Dawson’s seminal work proved that these superimposed deflections were of cortical origin. It was not until 1969 however, that

Herbert Vaughan actually coined the term that we all use today, “event-related potential” (ERP). EEG signals typically range from 10-100uV, whereas ERP deflections ranges from 3-6 uV. ERP components are displayed as a deflection of positive or negative polarity, labeled as P or N components respectively. Polarities detected along the scalp depend on several factors such as the type of neurotransmitters (excitatory or inhibitory), source(s) of the signals, and position of reference electrode(s). In the absence of detailed information about the underlying neural activity, the polarity of a signal has no direct physiological or functional significance.

ERPs are thought to result from stimulus-evoked brain activity and/or stimulus-induced changes in brain dynamics (Makeig et al. 2002; Pfurtscheller and da Silva 1999). A large number of studies have suggested that ERPs could be due to both phase-resetting of ongoing EEG oscillations and the increase of neuronal activations that are additive and independent of ongoing EEG oscillations (Fell et al. 2004; Shah et al. 2004). Event-related responses could be measured in amplitudes, representing the change in mean firing rates of neuronal populations or changes in the power of specific frequencies, representing the amount of neuronal synchrony. The two theories behind ERP formation are the evoked model and phase-reset model (Shah et al. 2004, Fell et al. 2004). The evoked model is based on the idea that populations of neural activity are evoked due to an event/stimulus, which will create an additive response and cause a power increase in the dominant frequency. The phase-reset model is based on the idea that there is a synchronization of neurons, phase resetting or phase locking of neurons, that does not change the actual amount of activated neurons. The phase-reset model will show a phase concentration in addition to a power increase that occurs outside of the dominant frequency. This power increase is serving as a change to assist in phase locking after the event/stimulus. Studies by Fell et al. (2004) and Shah et al. (2004) concluded that both phase concentration and power increases

contribute to the formation of ERPs, but to a different extent, depending on the task and varying conditions of the task.

One of the most extensively studied ERP components is the P300. The P300 is commonly detected with a positive polarity and peaking around 300 ms after stimulus. The P300 is commonly divided into two subcomponents: P3a and P3b (Coles and Rugg 1996 and Luck 1996). The P3b, also known as the classic P300, could be elicited by the popular 2-stimulus oddball paradigm. This paradigm consists of frequent “non-target” stimuli and infrequent “target” stimuli. The P3b is elicited only if the target stimuli is related to the task of the experiment. This component is strongest in the parietal region and often used to test cognitive loading because the P3b has been shown to change in amplitude and/or latency depending on changes in cognitive demands of the task (Luck 1996). The P3a, on the other hand, is known as the deviant P300 because this component could be elicited with a deviant stimuli, even if the stimuli is not related to the task at hand (unlike P3b). The P3a usually occurs at an earlier time than the P3b and is strongest in the frontal region. A task commonly used to elicit the P3a is the 3-stimulus oddball paradigm, where an additional infrequent third stimuli, the “deviant” stimuli, is included in the task. This P3a, similar to the CNV, could be habituated with repeated exposure to the deviant stimuli.

EEG has become a popular tool in neurophysiological and cognitive research because of its ability to record brain activity at a high temporal resolution. The functional mapping of the human brain provides a means to identify both the temporal and spatial characteristics of brain activity, providing clues to the underlying mechanisms behind the activation pattern. However, one of the shortcomings with EEG is its poor spatial resolution. EEG is recorded at the scalp with electrodes that are commonly clipped onto a cap worn by the subjects. Signals from within

our brain have to travel through many tissue layers (i.e. skin, scalp, skull, and brain) before reaching to the electrode surface. This volume conduction not only attenuates the signal but creates difficulty in identifying the precise location or source of the signal from within our brain, also called the inverse problem. There is no unique solution to this because the distribution of scalp potentials can be produced by many combinations of generator source(s). Therefore, we have to rely on models to predict the localization of these source(s). The extent of volume conduction and assumptions made by different models could be affected by source location, source configurations, and head properties. One common model used to estimate the source of brain potential is low-resolution electromagnetic tomographic analysis (LORETA) (Pascual-Marqui 2002). Recent research indicates that LORETA is among the more accurate and conservative approaches (Thatcher 2005). LORETA solutions are characterized with the assumption that there are highly synchronized activity among neighboring neurons and that the smoothest of all possible distributions is the most plausible to explain the data (Pascual-Marqui et al. 2002). In order to simplify the extensive calculations involved with determining the possible source(s) from recorded EEG signals, a forward model is performed prior to determining the inverse solution. The forward problem involves computing the scalp potentials at a finite set of source locations based on the assumptions made about source configuration and head properties. For example, the finite element model, FEM, is a volume-based modeling technique that considers individual anisotropic conductivities of each tissue type (skin, skull, and brain/CSF) in order to determine the solutions to the forward model.

CHAPTER 2
**SPATIOTEMPORAL DYNAMICS OF BRAIN ACTIVITY
DURING THE TRANSITION FROM VISUALLY GUIDED
TO MEMORY GUIDED FORCE CONTROL**

2.1. Introduction

Many daily activities require humans to produce force or perform movements with visual feedback and then transition to performing a similar motor output without visual feedback. One example is while driving a car, when an individual applies a force to the accelerator to maintain car speed and applies forces to the steering wheel to keep the car position within the lanes. The driver receives visual feedback of the other cars and the road ahead. At times however, the driver's eyes may transition away from the road to either pick up a drink or change the radio station, but the voluntary forces applied to the steering wheel and accelerator must be maintained.

Prior studies have found that the production of accurate force output depends on whether or not visual information is available (Slifkin et al. 2000), and on the amount of visual information available (Vaillancourt et al. 2006a). Visually guided force control tasks have been associated with activity in frontal and parietal cortices (Grol et al. 2007; Jeannerod et al. 1995; Kuhtz-Buschbeck et al. 2001). Ehrsson and colleagues (2001) identified several areas of the frontal and parietal cortices active during precision grip force control, including primary motor cortex, premotor cortex, supplementary motor area, cingulate motor area, and intraparietal cortex. Neuroimaging techniques that include positron emission tomography (PET) and functional magnetic resonance imaging (fMRI) have identified the anatomical regions that are activated during memory guided motor tasks (Cohen et al. 1997; Debaere et al. 2003; Jahanshahi et al. 1995; Mueller et al. 2007; Vaillancourt et al. 2003). The neural processes that underlie the

generation of memory guided force control have been specifically linked to the dorsolateral prefrontal cortex, ventral prefrontal cortex, and anterior cingulate cortex during isometric grip force control using fMRI (Vaillancourt et al. 2003). Studies using electroencephalography (EEG) have investigated memory processes within long delay periods of memory retention (Bender et al. 2010; Sauseng et al. 2002). However, the neural circuits that are utilized during the immediate transition from visually guided to memory guided force control have not been well elucidated.

It is well established that the prefrontal cortex is a key brain region that is involved with memory guided tasks. Neurophysiological studies in monkeys (Fuster and Alexander 1971; Kubota and Niki 1971; Miller et al. 1996) and fMRI studies in humans (Cohen et al. 1997; McCarthy et al. 1996) report persistent neuronal activity in the prefrontal cortex during the delay period of a working memory task. Lesions studies in monkeys and humans indicate that lesions to the prefrontal cortex impair working memory (Curtis and D'Esposito 2004; Müller and Knight 2006). Vaillancourt and colleagues (2003) were able to isolate memory-related processes to the prefrontal cortex during a precision grip force task using fMRI by separating motor memory processes from visual only and motor only activations. Studies using transcranial magnetic stimulation (TMS) over the dorsolateral prefrontal cortex (DLPFC) (Hamidi et al. 2009; Mottaghy et al. 2002; Oliveri et al. 2001; Postle et al. 2006) further confirms the role of the prefrontal cortex in working memory. A recent study using EEG examined the delay phase during a memory-guided saccade task and localized prefrontal activity only during the initial part of the delay period (Brignani et al. 2010). The extent and potential timing that prefrontal cortex is activated during the immediate transition from a visually guided motor task to a memory guided motor task is still not well established. Determining the relative timing of prefrontal

activation is an important step towards revealing the specific contribution of prefrontal areas during motor memory tasks.

The current study examines force performance and the spatiotemporal pattern of brain activity that occurs during the transition from a visually guided to a memory guided force control task using event-related potentials (ERPs) and low resolution electromagnetic tomography (LORETA). In accordance with the previously mentioned studies on the role of prefrontal cortex during accurate memory maintenance, we hypothesize that prefrontal event-related activity changes during the transition from visually guided to memory guided force control. Previous behavioral work suggests that the temporal capacity of short-term visuomotor memory can extend up to 2 s (Binsted et al. 2006; Elliott and Madalena 1987) or even shorter between 0.5-1.5 s during force production (Vaillancourt and Russell 2002). As such, we expect to observe behavioral changes between 0.5-1.5 s during the subjects' memory guided force production, and further predict that prefrontal activity changes before changes in behavior.

2.2. Research Design and Methods

2.2.1. Subjects

Twelve healthy right-handed subjects with normal or corrected vision participated in this study (6 females, aged 19-34 years; $M = 23.5$, $SD = 4.47$). Self-reported measures of handedness and medical history were used. Subjects were asked not to consume any caffeine and refrain from using any hair products on the day of testing. All subjects provided informed consent prior to the experiment. This study was approved by the local Institutional Review Board and in accordance with the Declaration of Helsinki.

2.2.2. Experimental design

Subjects sat up-right in a chair with their right forearm supported by a rigid arm rest and their thumb and index finger in a pinch grip position against two force transducers (Measurement Specialties, Hampton, VA) (Figure 2.1A). The experiment was carried out in a normally illuminated room with a computer monitor that was placed ~130 cm (52 in.) in front of the subjects. Before the experimental task, subjects performed three 3 s trials of maximal isometric pinch grip force. The largest force output of the 3 trials was used as the individual's maximal voluntary contraction (MVC). Next, each subject performed 5 practice trials that consisted of 20 s of rest followed by 30 s of force production at 15% of their MVC. Subjects were asked to practice a pinch grip force task so that: 1) the subjects can be familiarized with the equipment and general requirements of the study, and 2) the visual display during force production could be recorded and reproduced onto the screen for the subjects during a vision only condition of the task.

Figure 2.1B shows one experimental trial with the following sequence of conditions: 1) rest (R, 5s), 2) vision only with no force production (V, 6s), 3) force with visual feedback (FV, 5s), and 4) force from memory (FM, 4s). Each condition is described in further detail below:

1) R: Subjects were asked to rest and look straight ahead at the computer screen. A yellow stationary target bar was displayed and set at 15% of the subjects' MVC. A white stationary force bar was also displayed during the rest condition.

2) V: Subjects were asked not to produce any force and to focus their attention on the screen as the yellow target bar turns green and the white force bar fluctuates in real time according to the reproduction of the subjects' force output during practice trials. Subjects were asked to continue looking straight ahead at the screen as the white force bar disappears and only the green target

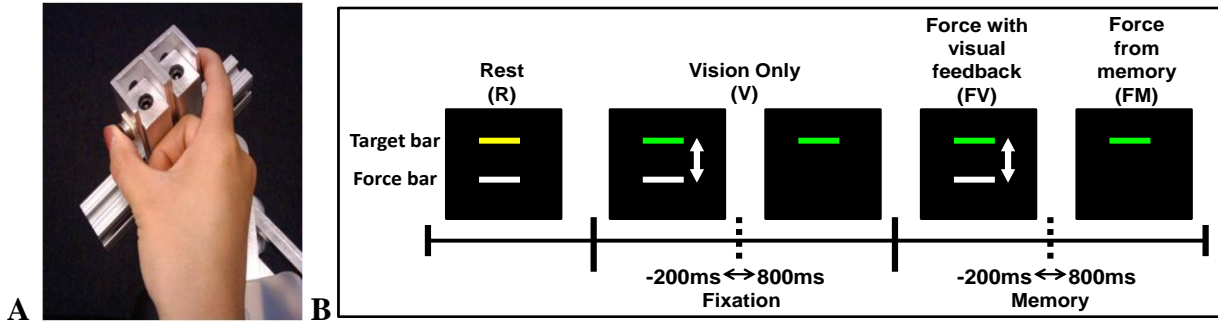


Figure 2.1. A: precision grip apparatus pressed with the subject's thumb and index fingers. B: sequence of conditions for each trial along with the visual display viewed by the subject. The transition periods that were examined are also shown.

bar remains on the screen. This is a reproduction of the same visual stimulus that subjects observed during force with visual feedback (FV) and force from memory (FM) conditions.

3) FV: Subjects were asked to produce force at 15% of their MVC when the white force bar reappears, matching the white force bar to the green target bar using online visual feedback of the force output.

4) FM: Subjects were asked to continue producing the same amount of force from memory after the white force bar disappeared.

Each trial lasted 20 s, with the trials repeated 25 times in one block. Each trial started in the same order of conditions as described above. To minimize a possible increase in electrocortical activity due to muscle fatigue (Johnston et al. 2001), subjects received a break of at least 3 minutes after every block in addition to R and V conditions that required no force production within each trial. A total of 8 blocks, equaling 200 trials, were performed by each subject. Subjects were instructed to minimize blinking during V, FV, and FM conditions. Because the focus of this study was on the *transition* from visually guided to memory guided force control, the analyses were focused on the transition within V and from FV to FM. The transition during V conditions will be referred to as the *fixation* transition. The transition from FV to FM will be referred to as the *memory* transition (Figure 2.1B). The fixation transition served as a control task for this study where subjects viewed an identical visual stimulus to that observed during the memory transition. This allowed us to parse out the neural activity associated with stimulus-related perception and isolate the neural activity relating to memory guided force control.

2.3. Data Acquisition and Statistical Analysis

2.3.1 Behavioral data acquisition

The force transducers used were ELFF-B4 model load cells constructed from piezoresistive strain gauges measuring force up to 100 N (Measurement Specialties, Hampton, VA). Force data was collected by Coulbourn Instruments Type B V72-25B amplifiers at an excitation voltage of 5 V. The force signal was transmitted via a 16-bit A/D converter and digitized at 200 Hz. The output from the force transducers was presented to the subject using a visual display on the computer screen (force bar in Figure 2.1B). The force output was displayed on the screen at a resolution of 1024x768 pixels and a refresh rate of 60 Hz. Digital triggers identifying the start of each condition (ie. R, V, FV, and FM) were sent from a program written in Labview to the Biosemi ActiveTwo acquisition software.

2.3.2. Electrophysiological data acquisition

The electroencephalogram (EEG) was collected using Biosemi ActiveTwo system with 128 Ag-AgCl Active Two electrodes. The active electrodes were connected to a cap that was configured very similarly with the 10-5 electrode system (Oostenveld and Praamstra 2001). One of three cap sizes was selected for the subjects depending on their head circumference (ie. 50-54 cm, 54-58 cm or 58-62 cm). Figure 2 shows the configuration of the electrodes. The signals were amplified through the electrode at the source and have an output impedance of less than 1 Ω . EEG signals were digitally amplified at DC and sampled at 2048 Hz. Electrical potentials were recorded between each electrode and the common mode sense (CMS) electrode, that is analogous to a ground. The CMS and a driven right leg (DRL) electrode are located towards the

center of the other electrodes as seen in Figure 2.2 (black-filled circles). The CMS and DRL electrodes were used to drive the average potential of the patient as close as possible to the AD-box reference potential electrode. The electrode offsets, a running average of the voltage measured between the CMS and each active electrode, were evaluated before the start of each block and during data collection to be within the acceptable range of ± 40 mV (BioSemi B.V., Amsterdam). The electrode offset served as an indirect measure of impedance tolerance to ensure that a stable and high quality signal was recorded from each active electrode.

2.3.3. Behavioral data analysis

Individual force trials were first visually inspected using a custom-written program in LabView to ensure that subjects were completing the requirements of the task (i.e. producing force during memory transitions and not producing force during fixation transitions). Trials were discarded from further analysis if force production was not completed as instructed. The force data was low-pass filtered using a fourth-order dual-pass Butterworth filter at 10 Hz. Force output was examined in 100 ms time bins from 200 ms before to 800 ms after the force transitions. Four dependent measures were calculated: 1) mean force output, 2) standard deviation (SD) of force, 3) coefficient of variation (CV) of force, and 4) the root mean squared error (RMSE) of the force in newtons. The RMSE reflected how accurate force production was relative to the target force output. The effect of time on force output was analyzed with repeated measures ANOVA using Greenhouse-Geisser corrections. Significance was determined with a p-value of less than 0.05. Significant effects were followed by Tukey's Honestly Significant Difference test to determine the first 100 ms time bin that was significantly different after visual feedback was removed.

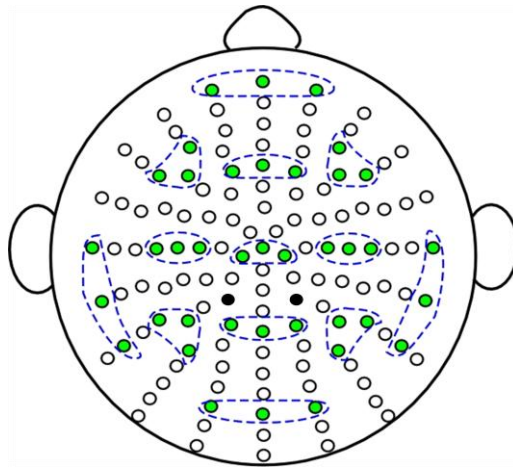


Figure 2.2. Clusters of 3 electrodes (*gray-filled circles*) are highlighted with dashed lines showing the 13 regions of interest (ROIs). Black-filled circles are the two reference electrodes used during data collection.

2.3.4. Electrophysiological analysis

All EEG data were imported into EMSE software suite (Source Signal Imaging, San Diego, CA) for analysis. The data was first re-referenced to a common average reference. The average reference was chosen to provide the best approximation of an absolute reference with a net source of zero (Srinivasan et al. 1998). This will also allow us to avoid the violation of quasi-stationarity for source estimation (Michel et al. 2004). Slow drifts within EEG signals were removed by polynomial detrend and baseline corrected to DC offset. Next, channels were band-pass filtered at 0.5-70 Hz. Then signals were downsampled from 2048 Hz to 512 Hz. Trials were manually inspected for movement and eye artifacts and discarded from further analyses if they contained visible artifacts. In addition, clear instructions were provided to subjects to fixate and focus on the force and target cursor on the screen, therefore horizontal eye movements were minimized. Vertical eye blinks and movements were carefully examined during individual inspection of each trial and trial acceptance was conservative. An average of 3 individual noisy channels was corrected with the EMSE spatial interpolation filter in 8 of the 12 subjects. The specified channels were recreated by interpolation using all other channels in the file and weighted as a function of its distance from the channel to be reconstructed. The average number of valid trials per subject was 149 trials (SD= 36.27) for the fixation transitions and 154 trials (SD= 35.9) for the memory transitions.

As we were interested in the transition period, the event-related potentials (ERPs) were extracted by averaging across all valid trials for each subject from 0 to 800 ms after the fixation and memory transitions (Figure 2.3). The transitions were carefully designed to control for the visual properties of the stimuli and to exclude neural activity relating to motor output production by removing visual feedback during the maintenance of force production. A total of eight 100

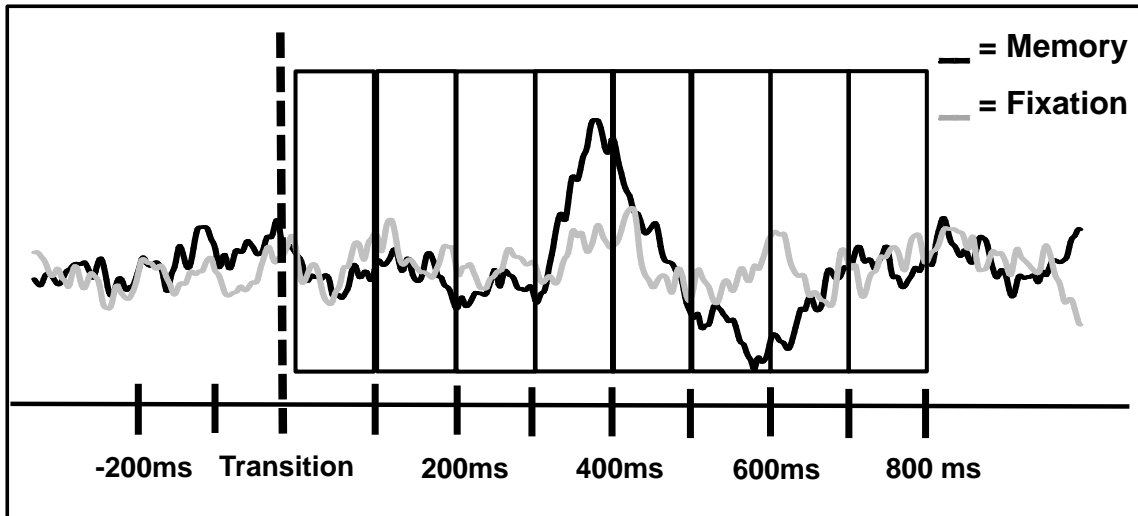


Figure 2.3. The eight 100ms time bins used to compare between fixation and memory transitions.

ms time bins were analyzed. The effect of time and transition on each region of interest (ROI) was analyzed using separate 2-way repeated measures ANOVA with Greenhouse-Geisser corrections (8 time bins x 2 transitions). ROIs were selected based on standardized positions of the international 10-5 system. The ROIs covered frontal (Fpz, F3, Fz, F4), central (C3, Cz, C4), parietal (P3, Pz, P4), temporal (T7, T8), and occipital (Oz) regions. Each ROI consisted of an average cluster of 3 electrodes. The two levels of transitions were examined across the eight 100ms time bins (Figure 2.3). Each significant time*transition interactions was followed with individual t-tests and corrected for multiple comparisons using Bonferroni corrections. For each interaction, a total of 8 t-tests were conducted and considered significant with a p-value < 0.00625. Electrophysiological results will be reported in terms of positive or negative polarities but no inferences will be made regarding the nature of the polarities, i.e. the structure and orientation of dipole(s) or the type of post-synaptic cells (excitatory or inhibitory).

2.3.5. Source analysis

In order to further understand the spatial pattern of brain activity during visually guided to memory guided force control, we performed source localization on the time bins that were 1) significantly different in the electrophysiological analysis, and 2) observed prior to behavioral changes in force output. Hence, low-resolution electromagnetic tomographic analysis (LORETA) was applied at each 100 ms time interval from 300 to 600 ms after the memory transition. The difference wave obtained by subtracting the grand-averaged event-related response during the memory transition from the fixation transition was used to compute three-dimensional linear solutions to the inverse problem within the constraints of a realistic finite element modeling (FEM) of an average brain (EMSE® Suite). FEM is a volume-based

modeling technique that considers individual anisotropic conductivities of each tissue type (skin, skull, and brain/CSF) to determine the solutions to the forward model. The distribution of neuronal generators as a current density value at each voxel and spatial resolution of 5 mm was determined. LORETA solutions are characterized with the assumption that there are highly synchronized activity among neighboring neurons and that the smoothest of all possible distributions is the most plausible to explain the data (Pascual-Marqui et al. 2002). Human Motor Area Template and prior fMRI studies from our laboratory were used to identify brain regions from the LORETA solutions (Mayka et al. 2006; Vaillancourt et al. 2003).

2.4. Results

2.4.1. Behavioral results

The target force level across subjects ranged from 3.9-12.75 N with the mean target force = 7.23 N (SD = 2.32). The analyses examined the dependent measures in consecutive 100 ms time bins from 200 ms before to 800 ms after visual feedback was removed in the force transition. Repeated measures ANOVA for mean force output was not significantly different indicating that mean force did not change across time [$F(9,99) = 1.65, p = 0.22$] (Figure 2.4A). SD and CV of force were also not significantly different across time [$F(9,99) = 0.96, p = .44$; $F(9,99) = 0.934, p = 0.45$] (Figure 2.4B and 2.4C). These results indicate that force variability did not change over the examined time bins. However, the root mean squared error (RMSE) of force production was significantly different across time [$F(9,99) = 18.53, p = 0.000025$] (Figure 2.4D). Tukey's Honestly Significant Difference test was subsequently used to detect the earliest time bin that was significantly different from 200 ms before visual feedback was removed. A

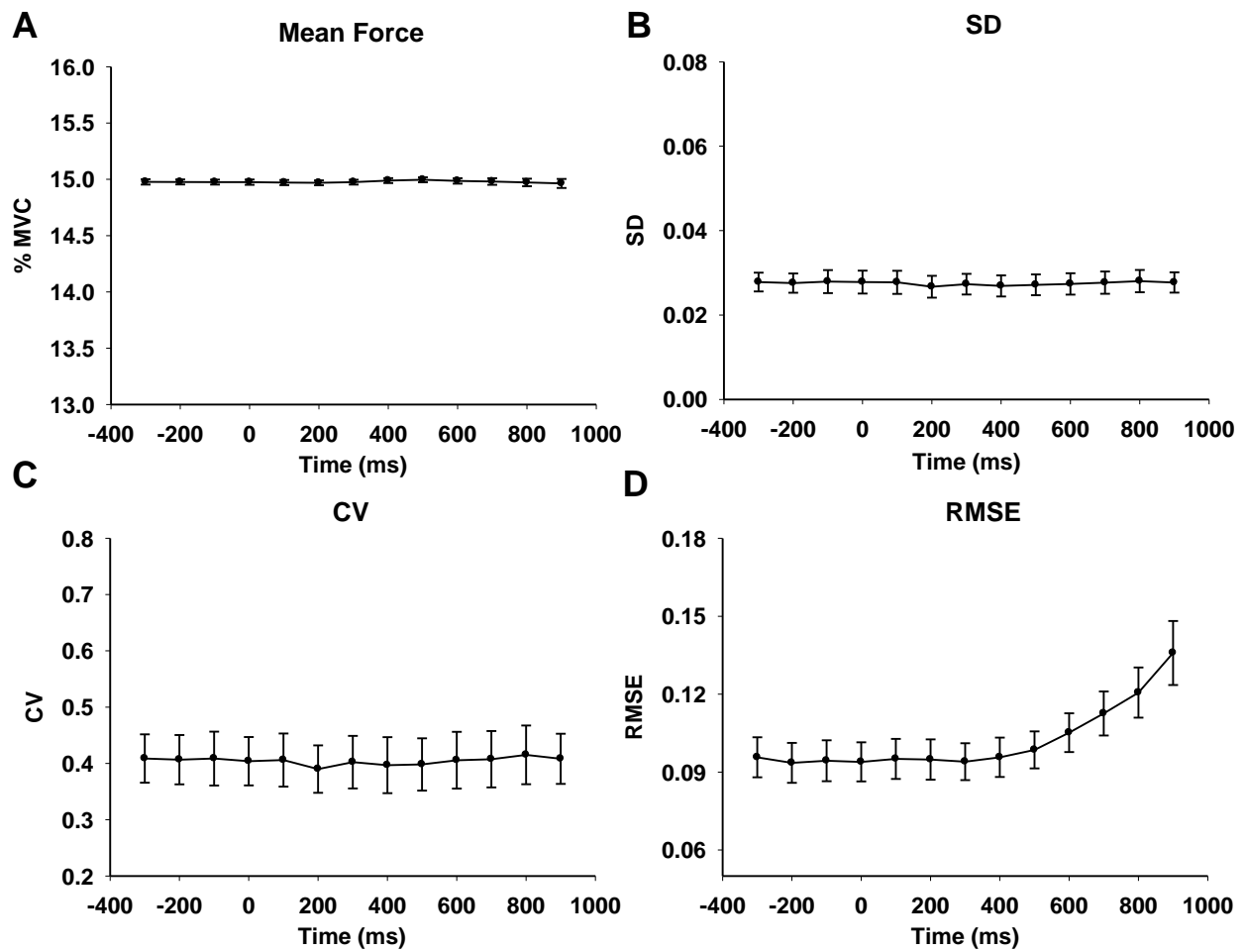


Figure 2.4. A: Subject's mean force output before and after visual feedback was removed. B: Standard deviation (SD) and C: Coefficient of variation (CV) of force. D: Root mean squared error (RMSE) of force production relative to the target force following the removal of visual feedback.

significant increase in force error was detected at 600 ms after visual feedback was removed. Thus, subjects were able to maintain force accuracy for at least 600 ms following the removal of visual feedback.

2.4.2. Electrophysiological results

Figure 2.5 illustrates the ERP topography map of the grand-average across all 12 subjects. The potential distribution is projected onto a standardized head shape. The visual stimulus (i.e. disappearing white force bar) initiated during both the fixation and force transitions resulted in a similar pattern of visual ERP components between 0 and 300 ms. Next, a centrally-distributed positivity was observed between 300 and 400 ms in the force transition but not the fixation transition. This was followed by a prefrontal positivity between 400 and 600 ms in the force transition. A centrally-distributed negativity could also be seen between 400 and 600 ms in both transitions. Lastly, a frontal negativity and parietal positivity could be observed in both force and fixation transitions with the negative component appearing earlier between 400 and 500 ms, followed by the positive component between 500 and 600 ms. This frontal-negative and parietal-positive pattern persisted for the remainder of the examined time bins in both transitions.

Significant time*transition interactions were found in 7 of the 13 ROIs (i.e. Fpz, F3, F4, C3, Cz, P3, and Pz channel groups) (Table 2.1), followed by significant t-tests in 6 of the 7 significant interactions after Bonferroni corrections (i.e. Fpz, F3, F4, C3, P3, and Pz channel groups) (Figure 2.6). This suggests that ERPs, relating to the maintenance of force production and not the visual stimulus, were detected in these regions. Detailed results of the statistical analyses can be found in Table 2.1. Post-hoc t-tests revealed that significant differences occurred as early as 300 ms after the removal of visual feedback. The green box in Figure 2.6

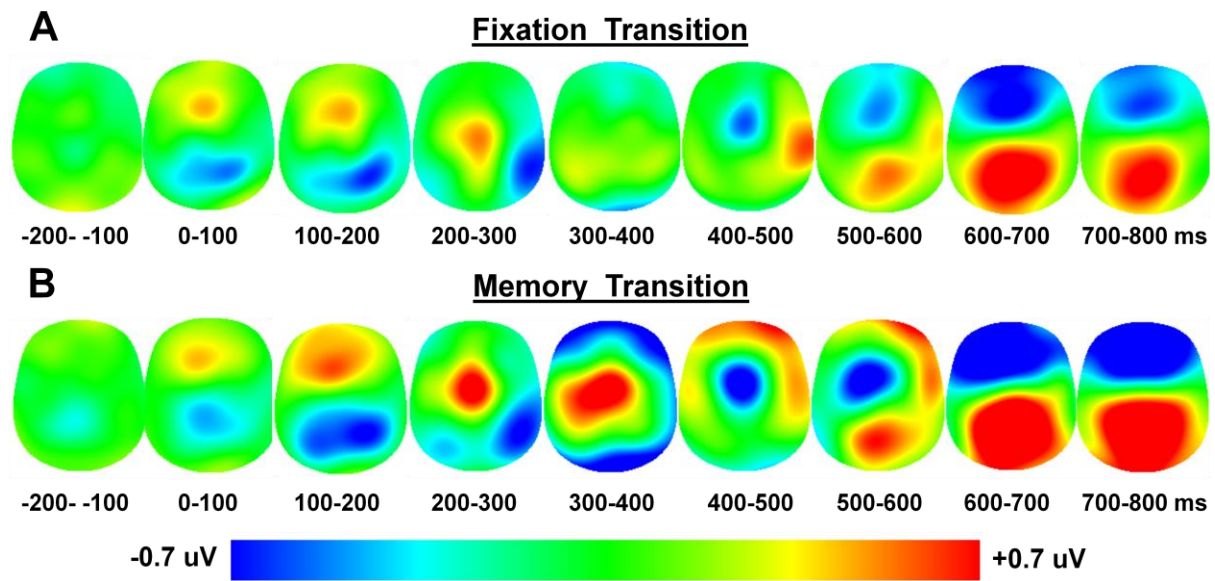


Figure 2.5. Grand-average event-related topography in 100 ms time bins from -200 ms to 800 ms after (A) fixation transition and (B) memory transition.

shows the first region with significant changes in ERPs was detected over the C3 channel group, contralateral to the hand producing force (also see Table 2.1). By 400 ms after visual feedback was removed, significant differences were found in the Fpz channel group and this is highlighted in the yellow box in Figure 2.6. The prefrontal activity along with the centrally-located C3 channel group, were simultaneously significant from 500 to 600 ms after visual feedback was removed. Lastly, a significant change in ERPs occurred across bilateral frontal and left parietal cortices (F3, Fz, F4, P3, and Pz channel groups) at 700 ms after visual feedback was removed. As shown in the red boxes in Figure 2.6, this simultaneous frontal-negativity and parietal-positivity can be observed more prominently during the memory transition than the fixation transition (also see Figures 2.5).

2.4.3. Source results

The results of the source analysis for Experiment 1 can be seen in Figure 2.7. Specific brain regions corresponding to the observed solutions are overlaid onto an average brain included in the EMSE suite and distributed with the SPM (Statistical Parametric Mapping) software made available by the Wellcome Department of Imaging Neuroscience at University College London, UK. The more intense red color indicated a greater source of activation from the specific regions. The solution illustrated a stronger focus of activity in the left ventral premotor cortex from 300 to 500 ms after memory transition. Maximum current density values were identified at ($X = -54$, $Y = 4$, $Z = 9$) from 300 to 400 ms and ($X = -54$, $Y = 8$, $Z = 11$) from 400 to 500 ms after visual feedback was removed, both representing Brodmann's area (BA) 6 in Talairach coordinates. Maximum activation from 500 to 600 ms after visual feedback removal

was localized to the right ventral prefrontal cortex at (X = 24, Y = 48, Z = -6) corresponding to BA10/11.

Table 1 Experiment 1 ANOVA results for condition by time interaction and follow-up t-tests

Location of channel groups	F-value	Epoch (ms)		100 to 200		200 to 300		300 to 400		400 to 500		500 to 600		600 to 700		700 to 800		
		t	p	t	p	t	p	t	p	t	p	t	p	t	p	t	p	
Fpz	4.52	0.009	0.86	0.79	0.44	-0.33	0.75	-1.56	0.15	3.60	0.004	4.57	8E-04	0.004	0.99	-2.29	0.04	
F3	4.84	0.003	0.72	0.49	2.03	0.07	0.96	-1.90	0.08	2.13	0.06	0.94	0.37	-2.97	0.01	-3.69	0.004	
Fz	2.46	0.070																
F4	6.80	4E-04	1.31	0.22	2.70	0.02	-0.16	0.87	-2.50	0.03	1.82	0.10	2.61	0.02	-1.81	0.10	-4.26	0.001
C3	5.52	0.002	-0.10	0.93	-1.27	0.23	0.61	0.55	4.66	7E-04	0.43	0.68	-3.73	0.003	-1.20	0.26	-0.32	0.76
Cz	5.10	0.008	-1.14	0.28	-1.02	0.33	2.85	0.02	2.91	0.01	-2.23	0.05	-2.05	0.07	0.66	0.52	0.10	0.92
C4	0.40	0.765																
T7	1.20	0.330																
P3	4.94	0.003	-0.76	0.46	-3.09	0.01	-1.08	0.30	1.72	0.11	0.53	0.61	-1.50	0.16	2.63	0.02	5.63	2.E-04
Pz	4.97	0.005	-0.51	0.62	-3.10	0.01	-1.45	0.17	1.63	0.13	-1.78	0.10	-0.72	0.49	2.56	0.03	3.49	0.005
P4	2.23	0.095																
T8	1.20	0.320																
Oz	2.14	0.120																

2-way repeated measures ANOVA (8 time bins by 2 transitions) was performed. Corresponding F-values and Greenhouse-Geisser corrected p-values are shown. Each significant interaction was followed up with individual t-tests and considered significant with a Bonferroni corrected p-value < 0.00625. Corresponding t-values and p-values are shown. ROIs with significant interactions followed by significant t-tests are highlighted in bold. Significant p-values are highlighted in bold.

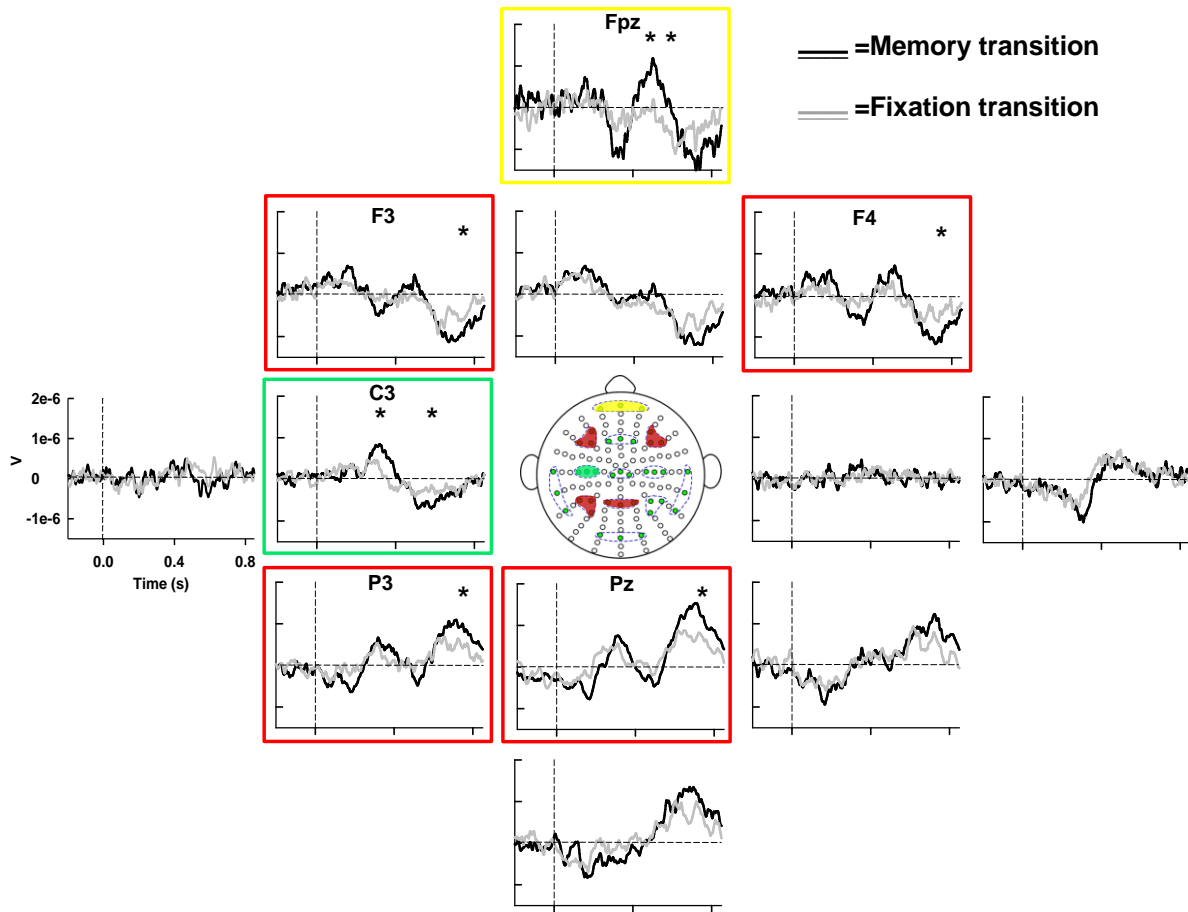


Figure 2.6. Grand-average event-related potentials (ERPs) of regions of interest (ROIs) in the memory transition (*black*) and fixation transition (*gray*). Statistically significant ROIs are highlighted chronologically from earliest to latest time of significance (i.e. *green to yellow to red*). * indicates significant time bins within each ROI.

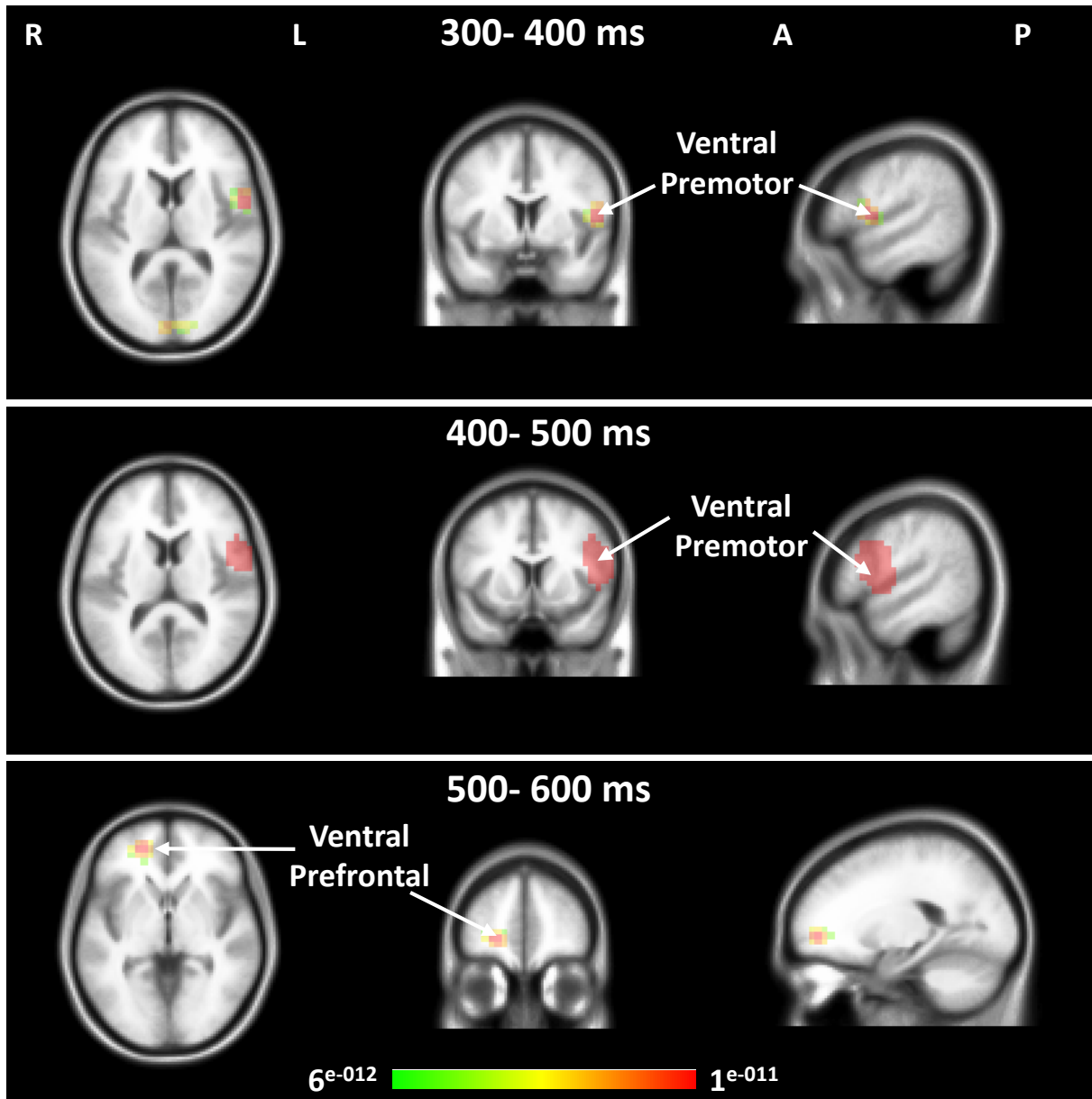


Figure 2.7. Grand-averaged ERP difference results of the LORETA analysis showing current density maxima from 300-400 ms (top row), 400-500 ms (middle row), and 500-600 ms time bins (bottom row). Each map consists of axial, coronal, and sagittal slices showing the same area of maximum activation.

2.5. Discussion

This study demonstrated the spatiotemporal pattern of brain activity during the transition from a visually guided to a memory guided force control task. The primary finding of this study is that early event-related changes in activity of the lateralized central (C3) and prefrontal (Fpz) regions are associated with memory guided continuous force production. These changes occurred before any changes in behavior were detected. Further tomographical analysis (LORETA) confirmed that the most prominent and consistent sources of activity were localized to the left ventral premotor cortex (BA6) and right ventral prefrontal cortex (BA10/11). Our findings show that subjects rely on early and rapid sensorimotor memory processes involving the ventral premotor cortex and ventral prefrontal cortex.

2.5.1. Premotor activation

One of the novel findings in this study is that the first event-related activity was observed as early as 300 ms in the left central region (C3 channel group) after visual feedback was removed. Cortical localization (LORETA) indicated the left ventral premotor cortex (BA6) as the brain region primarily responsible for the observed event-related activity between 300 and 400 ms after visual feedback was removed. In addition to its well-established motor function, the premotor cortex has been associated with working memory processes (D'Esposito et al. 1998; Jonides et al. 1993; Owen et al. 2005). Premotor activation has been recorded during delayed-response memory tasks in humans (Baker et al. 1996; Jonides et al. 1993; Mecklinger et al. 2002). These prior studies have associated premotor activation with motor preparation and attention towards the target during a delayed response memory condition. Another fMRI study was able to show ventral premotor activation contralateral to the dominant hand while retaining

information about objects that require future motor actions (Mecklinger et al. 2004). Our result extends previous evidence to ventral premotor cortex involvement during the active maintenance of motor requirements from memory.

The observed left-lateralized central positivity during memory guided force control can also be related to the P300 component. The act of switching from a visually guided task to a memory guided task could be related to the classic central-parietal P300 component that was proposed to reflect context updating and monitoring of working memory (Donchin 1981; Polich and Donchin 1988). A variety of studies have demonstrated changes in the topography of the P300 depending on the type of information processed in working memory (Lang et al. 1992; Mecklinger and Pfeifer 1996; Ruchkin et al. 1992) and changes in the amplitude of the P300 depending on the amount of information retained in working memory (Ruchkin et al. 1992). The observed scalp topography of a left-lateralized central P300 component in the current study is likely due to the fact that we studied a continuous motor memory task using the right hand whereas prior studies that observed a P300 component in the central-parietal cortex have focused on visual or auditory detection tasks (Picton 1992). Hence, our findings extend the previous evidence by showing a spatially specific centrally-located change in the P300 during the transition from visually guided to memory guided force production.

2.5.2. Prefrontal activation

Following the change in activity in the left central region, changes in the prefrontal cortex (Fpz channel group) were identified as early as 400 ms into the memory guided task. LORETA solutions identified the strongest source of brain activity from the ventral prefrontal cortex (BA10/11) between 500 and 600 ms after visual feedback was removed. One of the early

observations seen in monkeys was the sustained neural activity within the prefrontal cortex during the delay period of a delayed-response task (Fuster 1973; Fuster and Alexander 1971). This prefrontal activity is also consistent with what has been previously identified in fMRI and PET studies during internally-generated movements (Jenkins et al. 2000; Vaillancourt et al. 2003). Involvement of the prefrontal cortex has been shown in studies describing the prominent role of this region in various forms of working memory (WM) (i.e. visual, auditory, and tactile memory) (Curtis and D'Esposito 2003; Gallace and Spence 2009; Postle 2006). LORETA solutions are in line with the results of neuroimaging and neurophysiological studies indicating the specific activation of ventral prefrontal cortex during working memory tasks (Inoue et al. 2004; Owen et al. 2005; Rosenkilde et al. 1981; Wager and Smith 2003). Another support for ventral prefrontal involvement during working memory processes is when delayed-response memory performance is impaired in individuals with ventral prefrontal lesions (Meunier et al. 1997; Oscar-Berman 1975). Barbey and colleagues (Barbey et al. 2011) recently demonstrated the critical role of the ventral prefrontal cortex during working memory tasks that require multiple higher-order cognitive processing such as the n-back task. Because subjects in the current study had to actively maintain and monitor the isometric force demands during the transition from visually guided to memory guided force control, our findings are consistent with Barbey and colleagues' study showing ventral prefrontal activity during tasks that require additional higher-order cognitive demands.

2.5.3. Frontal-parietal network of motor memory

The unique spatiotemporal pattern of brain activities observed in this study provides support for a network extending across the frontal regions, including the ventral prefrontal cortex

and ventral premotor cortex. These cortical areas could constitute part of a network that mediates motor memory processes. These results support previously identified connections of ventral prefrontal and premotor cortices with the dorsolateral prefrontal cortex and posterior parietal cortex during tasks requiring memory in non-human primates (Goldman-Rakic 1988; Selemon and Goldman-Rakic 1988). Although changes in parietal activity were not observed before behavioral changes occurred, we did observe changes in parietal activity by 700 ms after visual feedback was removed. This is in agreement with the strong basis of support for the dynamics between frontal and parietal cortices during memory guided tasks as shown through single-unit recordings in primates (Chafee and Goldman-Rakic 2000; Nieder and Miller 2004). Chafee and Goldman-Rakic (2000) confirmed the reciprocal projections between prefrontal and parietal regions through cortical cooling in one region and single-unit recording of the other region during a visuomotor working memory task. Prefrontal and parietal cooling led to a significant impact on the neuronal activity of parietal and prefrontal regions, respectively. The temporal order of prefrontal activity followed by parietal activity has been demonstrated in non-human (Tomita et al. 1999) and human studies (Brass et al. 2005; Bunge et al. 2002).

2.5.4. Summary

In summary, the high temporal resolution of EEG measures in combination with source localization provided novel insights into the spatiotemporal pattern of motor memory processing. This study demonstrates that subjects rely on sensorimotor memory processes during the absence of visual feedback that involves ventral premotor cortex and ventral prefrontal cortex. These changes in ventral premotor and ventral prefrontal activity occurred prior to changes in behavioral force error and prior to any changes in the mean force output. These findings suggest

that when subjects maintain force at a steady level shortly after the removal of visual feedback, they begin to rely upon specific neural processes in the premotor and prefrontal cortex. Since the premotor cortex and prefrontal cortex are affected by both aging and by specific neurological disorders, it is possible that our current findings may provide future insight into the timing and location that memory-guided motor output is affected with aging and neurological disease.

CHAPTER 3

SPATIOTEMPORAL DYNAMICS OF BRAIN ACTIVITY DURING ADAPTATION TO CHANGES IN VISUAL GAIN

3.1. Introduction

Visually-guided precision grip tasks depend on a visuomotor system consisting of parietal-frontal regions including the superior and inferior parietal cortex, premotor cortex, and primary motor cortex (Binkofski et al. 1999; Kuhtz-Buschbeck et al. 2001; Vaillancourt et al. 2003). Laboratory studies have also shown that amplifying the gain of visual signals enhances performance on tasks such as drawing (Prager and Contreras-Vidal 2003), force control (Newell and McDonald 1994a), and arm pointing (Seidler et al. 2001a). When the visual gain is increased, the spatial amplitude of the visual feedback changes on the display and this improves performance. Specific regions of the visuomotor system have been shown to respond selectively to different static levels of visual gain. When visual gain is increased at high gain levels, increased activation was observed in the dorsal and ventral premotor areas and inferior parietal lobule (Coombes et al. 2010a). On the other hand, when visual gain is increased at low gain levels, the same authors found increased activation in primary motor cortex, V3 and V5 of the extrastriate visual cortex, and ventral premotor cortex.

Although considerable focus has been given to how motor performance and brain activity changes during static changes in visual gain, less is known about the acute adaptation to increased visual gain. Does force variability decrease during the adaptation phase as has been shown during static changes in visual gain? Or, does force variability increase as the visuomotor regions of the brain adapt to the changes in visual gain. And, do the same brain circuits respond to changes in visual gain during the adaption phase as has been shown for static changes in

visual gain? The literature on adapting to visuomotor rotations offers some insight into how behavior and brain circuits respond to enhanced visual gain. Anguera and colleagues (2009) studied adaptations to visuomotor rotations and found that when subjects produced large errors, the magnitude of the event-related potential in frontal-central electrodes was greater as compared to when subjects made small errors. Also, Gentili and colleagues (2011) employed a visuomotor rotation task and found a prominent engagement of the frontal cortical regions that gradually diminished as the task was achieved. These authors also identified a relationship between movement error and electrical activity in frontal circuits. Collectively, these studies indicate that cortical activity changes during visuomotor adaptation and it is possible that visual gain could also cause changes in cortical activity. However, Krakauer and colleagues (2004b) used H_2^{15}O positron emission tomography (PET) to study adaptations to visuomotor transformations and visual gain. Although visuomotor transformations induced changes in the cortex, the authors found that only subcortical areas (putamen and cerebellum) responded with a change in relative cerebral blood flow to visual gain-related adaptations. The measurements observed with PET are over a long time scale (tens of seconds) and it is possible that the visual gain-related adaptations in the cortex occur over a short time scale.

Here, we sought to determine how increased visual gain influences motor performance and electrical brain activity in parietal-frontal regions through two experiments which manipulated the transition from low to high visual gain and high to low visual gain. Brain activity was monitored using high density electroencephalography (EEG) and source estimation was performed using low-resolution electromagnetic tomography (LORETA) during an isometric visually-guided grip force task. In contrast to a series of experiments from different laboratories which have examined static levels of visual gain and consistently found that high

visual gain leads to reduced force variability (Baweja et al. 2010; Beuter et al. 1995; Hong and Newell 2008; Stephens and Taylor 1974), we test the hypothesis that when subjects immediately adapt to a transition from low to high visual gain, there will be an acute increase in force variability as the visuomotor regions of the brain adapt to the novel visual stimulus. We also predict that increasing visual gain involves a shift in electrocortical activity within parietal-frontal circuits that will be systematically related to force variability. Finally, we expect that LORETA-based source localization will be consistent with prior fMRI studies which have localized visual gain-related changes to ventral and dorsal premotor cortex, extrastriate visual cortex, and parietal cortex (Coombes et al. 2010a).

3.2. Research Design and Methods

3.2.1. Subjects

A total of 11 subjects were in Experiment 1 (6 females, aged 19-30 years; $M = 22.73$, $SD = 3.82$) and 11 were in Experiment 2 (5 females, aged 19-30 years; $M = 23.45$, $SD = 3.80$). Ten of the 11 subjects participated in both experiments. All subjects were healthy right-handed subjects with normal or corrected vision. Subjects were asked not to consume any caffeine, refrain from using any hair products on the days of testing, and to wear prescription glasses instead of contact lenses for corrected vision. Informed consents were obtained from each subject prior to the experiment. This study was approved by the local Institutional Review Board and in accordance with the Declaration of Helsinki.

3.2.2. Experimental design

Subjects made two separate visits to the laboratory. One day consisted of subjects performing the low-to-high visual gain transitions (Experiment 1). Another day consisted of the subjects performing the high-to-low visual gain transitions (Experiment 2). The order of the experiments (i.e. low-to-high and high-to-low transitions) was counter-balanced between the subjects. Maximum duration between visits was 7 days. Subjects sat up-right in a chair with their right forearm supported by a rigid arm rest and their thumb and index finger in a pinch grip position against two force transducers (Measurement Specialties, Hampton, VA) (Figure 3.1A). The experiments were carried out in a dimly-illuminated room with a computer monitor that is placed ~130 cm (52 in.) in front of the subjects. Before the experimental task, subjects performed three 3 s trials of maximal isometric pinch grip force. The largest force output of the 3 trials was used as the individual's maximal voluntary contraction (MVC). Next, each subject performed 5 practice trials that consisted of 11 s of rest followed by 6 s of force production at 15% of their MVC. One trial from each subject's practice session was saved so that it could be reproduced onto the screen for the subject during the vision only condition of the experimental task (Figure 3.1B).

The subjects were required to maintain a steady isometric force output with a change in visual feedback gain level during force production. The visual gain can be varied by manipulating the distance of the eye to the computer monitor and/or changing the spatial amplitude of force output provided to the subject through a white cursor on the monitor. Spatial amplitude (α) could be affected by both the distance of the eye to the monitor or the force output size. In this study, the distance between the subject and the computer monitor is always kept constant, therefore visual gain was manipulated by changing the size of force output as viewed by the subject. Two visual gains were selected to ensure that we obtained a gain value above and

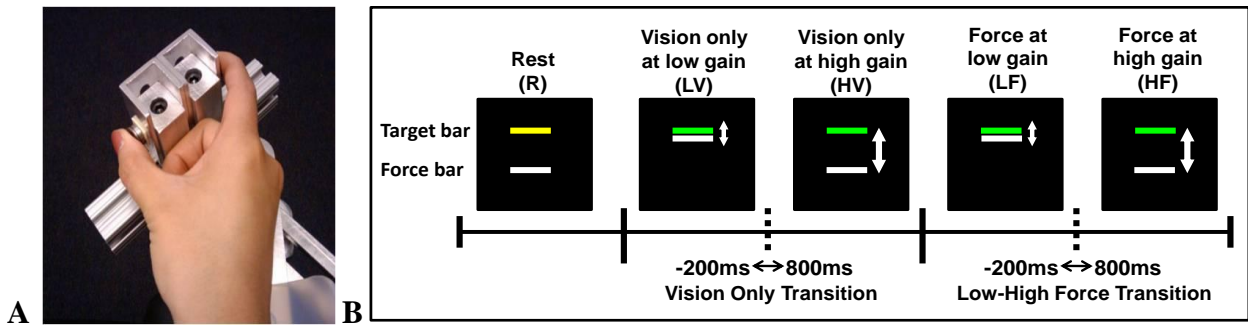


Figure 3.1. A: precision grip apparatus pressed with the subject's thumb and index fingers. B: sequence of conditions for each trial along with the visual display viewed by the subject. The transition periods that were examined are also shown.

below 1°, spanning the range across which a dramatic change in force performance will occur (Vaillancourt et al. 2006a, Coombes et al. 2010). The height of the force fluctuations viewed by the subject was manipulated using the following formula:

$$\text{White cursor position} = ((F_p - F_t) \times G) + F_t \quad (1)$$

in which F_p is the force produced by the subject, F_t is the target force, and G is the gain level used to change the spatial amplitude of visual feedback. Visual angle was calculated by assuming a set force output standard deviation (SD) of 0.3 N (Vaillancourt et al. 2006a). The full range ($\pm 3SD$) of the estimated variance for the height of force fluctuation was approximated by multiplying the SD value by 6 ($0.3N \times 6 = 1.8N$). The visual angle for each gain level was then calculated using the following formula:

$$\alpha = \arcsin\left(\frac{H_1}{D}\right) \quad (2)$$

in which α is the visual angle, D is the distance to the monitor, and H_1 is the height of the total range of motion in the top half of the visual field (Figure 3.2). The low and high visual gain levels correspond to visual angles of 0.026 and 2.908°, confirming that the selected visual angles were well below and above 1°, respectively. The two levels of visual gain will be referred to as low gain (0.026°) and high gain (2.908°) throughout the remainder of this study.

Each experimental trial was 20s long. The experimental trials consisted of the following conditions: 1) rest (R, 5 s), 2) visual only at low gain (LV, 3 s), 3) visual only at high gain (HV),

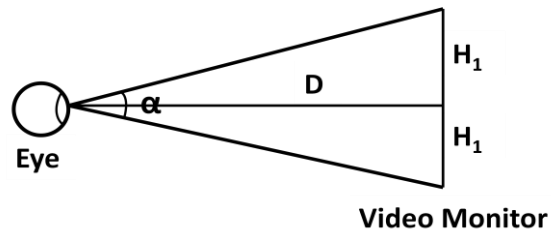


Figure 3.2. The calculation for visual angle was determined by the distance from the eye to the monitor, along with the height of the force fluctuations viewed on the computer monitor.

3 s), 4) force with visual feedback at low gain (LF), 5 s), 5) force with visual feedback at high gain (HF), 4 s) (Figure 3.1B). Note that there was no gap between these 5 conditions. Each condition is described in further detail below:

1) R: Subjects were asked to rest and look straight ahead at the computer screen. A yellow stationary target bar was displayed and set at 15% of the subjects' MVC. A white stationary force bar was also be displayed during the rest condition.

2) LV: Subjects were asked not to produce any force, but to focus their attention on the screen as the yellow target bar turns green and the white force bar fluctuates in real time according to a reproduction of the subjects' force output during a practice trial at low visual gain. This reproduction is a similar visual stimulus that subjects observed during force with visual feedback at low visual gain (LF).

3) HV: Subjects were asked to continue looking straight ahead at the screen as the white force bar switches to the high gain condition in real time according to a reproduction of the subjects' force output. The green target bar remained on the screen. This reproduction is a similar visual stimulus that subjects observed during force with visual feedback at high gain (HF).

4) LF: Subjects were asked to produce force at 15% of their MVC by matching the white force bar to the green target bar using online visual feedback of the force output set at the low gain level.

5) HF: Subjects were asked to continue matching the white force bar to the green target bar using online visual feedback of the force output set at the high gain level.

Trials were repeated 25 times in one block. A total of 8 blocks, equaling 200 trials, were performed by the subjects during each day of testing. Six of the 12 subjects performed Experiment 1 (low to high visual gain transition) on their first visit followed by Experiment 2

(high to low visual gain transition) on their second visit. The other 5 subjects performed Experiment 2 on their first visit followed by Experiment 1 on their second visit. Experiment 1 appeared in the following order of conditions: R, LV, HV, LF, and HF. Experiment 2 appeared in the following order of conditions: R, HV, LV, HF, and LF. Subjects were instructed to minimize blinking during LV, HV, LF, and HF conditions. Subjects also received a break of at least 3 minutes after every block of 25 trials to minimize fatigue.

Because the focus of this study is on the transition between changes in visual gain, the analyses focused on the transitions from LF to HF in Experiment 1 and HF to LF in Experiment 2. The transitions from LF to HF in Experiment 1 will be referred to as the *low-high force* transition. The transitions from HF to LF in Experiment 2 will be referred to as the *high-low force* transition. The transitions from LV to HV and HV to LV will be referred to as the *vision only* transitions. The fixation transitions served as a control where subjects viewed an identical visual stimulus to that observed during the gain transitions. This allowed us to parse out the neural activity associated with the visual stimulus and isolate the neural activity relating to the changes in visual gain.

3.3. Data Acquisition and Statistical Analysis

3.3.1. Behavioral data acquisition

The force transducers used were ELFF-B4 model load cells constructed from piezoresistive strain gauges with glass to stainless steel force measuring up to 100 N (Measurement Specialties, Hampton, VA). Force data was collected by Coulbourn Instruments Type B V72-25B amplifiers at an excitation voltage of 5 V. The force signal was transmitted via

a 16-bit A/D converter and digitized at 200 Hz. The output from the force transducers was presented to the subject using a visual display on the computer screen (force bar in Figure 3.1B). The force output was displayed on the screen at a resolution of 1024x768 pixels and a refresh rate of 60 Hz. Digital triggers identifying the start of each condition were sent from a program written in Labview to the Biosemi ActiveTwo acquisition software.

3.3.2. Electrophysiological data acquisition

The electroencephalogram (EEG) was collected using Biosemi ActiveTwo system with 128 Ag-AgCl Active Two electrodes. The active electrodes were connected to a cap that was configured very similarly with the 10-5 electrode system (Oostenveld and Praamstra 2001). One of three cap sizes was selected for the subjects depending on their head circumference (ie. 50-54 cm, 54-58 cm or 58-62 cm). Figure 3.3 shows the configuration of the electrodes. Each electrode was amplified through the electrode at the source and has an output impedance of less than 1 Ω . EEG signals were digitally amplified at DC and sampled at 2048 Hz. Electrical potentials were recorded between each electrode and the common mode sense (CMS) electrode, that is analogous to a ground. The CMS and a driven right leg (DRL) electrode are located towards the center of the other electrodes as seen in the figure (black-filled circles). The CMS and DRL electrodes were used to drive the average potential of the patient as close as possible to the AD-box reference potential electrode. The electrode offset, a running average of the voltage measured between the CMS and each active electrode, were evaluated before the start of each block and during data collection to be within the acceptable range of ± 40 mV (BioSemi B.V., Amsterdam). The electrode offset served as an indirect measure of impedance tolerance to ensure that a stable and high quality signal is recorded from the active electrodes.

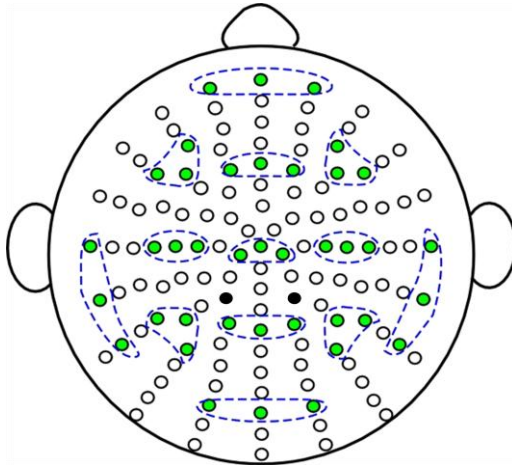


Figure 3.3. Clusters of 3 electrodes (*gray-filled circles*) are highlighted with dashed lines showing the 13 regions of interest (ROIs). Black-filled circles are the two reference electrodes used during data collection.

3.3.3. Behavioral data analysis

Individual force trials were first visually inspected using a custom-written program in LabView to ensure that subjects were completing the requirements of the task (ie. producing force during force transitions and not producing force during the vision only transitions). Trials were discarded from further analysis if force production was not completed as instructed. The force data was low-pass filtered using a fourth-order dual-pass Butterworth filter at 10 Hz. Force output was examined in 100 ms time bins from 200 ms before to 800 ms after the force transitions. Four dependent measures were calculated: 1) mean force output, 2) standard deviation (SD) of force, 3) coefficient of variation (CV) of force, and 4) the root mean squared error (RMSE) of the force in Newtons. This will reflect how accurate force production was relative to the target force output. The effect of time on force output was analyzed with repeated measures ANOVA using Greenhouse-Geisser corrections. Significance was determined with a p-value of less than 0.05. Significant effects were followed by Tukey's Honestly Significant Difference test to determine the 100 ms time bins that were significantly different after visual gain changes.

3.3.4. Electrophysiological data analysis

All EEG data were imported into EMSE software suite (Source Signal Imaging, San Diego, CA) for analysis. The data were first re-referenced to a common average reference. The average reference was chosen to provide the best approximation of an absolute reference with a net source of zero (Srinivasan et al. 1998). This will also allow us to avoid the violation of quasi-stationarity for source estimation (Michel et al. 2004). Slow drifts within EEG signals were removed by polynomial detrend and baseline corrected to DC offset. Next, channels were

band-pass filtered at 0.5-70 Hz. Then signals were downsampled from 2048 Hz to 512 Hz. Trials were manually inspected for movement and eye artifacts and discarded from further analyses if they contained visible artifacts or baseline drift. Trials were automatically excluded from averaging with a cutoff threshold set at ± 100 μ V. In addition, clear instructions were provided to subjects to fixate and focus on the force and target cursor on the screen, therefore horizontal eye movements were minimized. Vertical eye blinks and movements were carefully examined during individual inspection of each trial and trial acceptance was conservative. An average of 2 individual noisy channels were corrected with the EMSE spatial interpolation filter in 7 of the 11 subjects in Experiments 1 and 2. The specified channels were recreated by interpolation using all other channels in the file and weighted as a function of its distance from the channel to be reconstructed. For Experiment 1, the average number of valid trials per subject was 139 trials (SD= 22.99) for the vision only transitions and 165 trials (SD= 20.54) for the low-high force transitions. For Experiment 2, the average number of valid trials per subject was 121 trials (SD = 36.43) for the vision only transitions and 132 trials (SD = 36.3) for the high-low force transitions.

As we are interested in the transition period, the event-related potentials (ERPs) were extracted by averaging across all valid trials for each subject from 0 to 800 ms after the vision only and low-high force transitions in Experiment 1 and vision only and high-low force transitions in Experiment 2. The transitions were carefully designed to control for the visual properties of the stimuli and to exclude neural activity relating to motor output production by removing visual feedback or manipulating visual gain during the maintenance of force production. A total of eight 100 ms time bins were analyzed (Figure 3.4). For Experiments 1 and 2, the effect of time and transition on each region of interest (ROI) were analyzed using

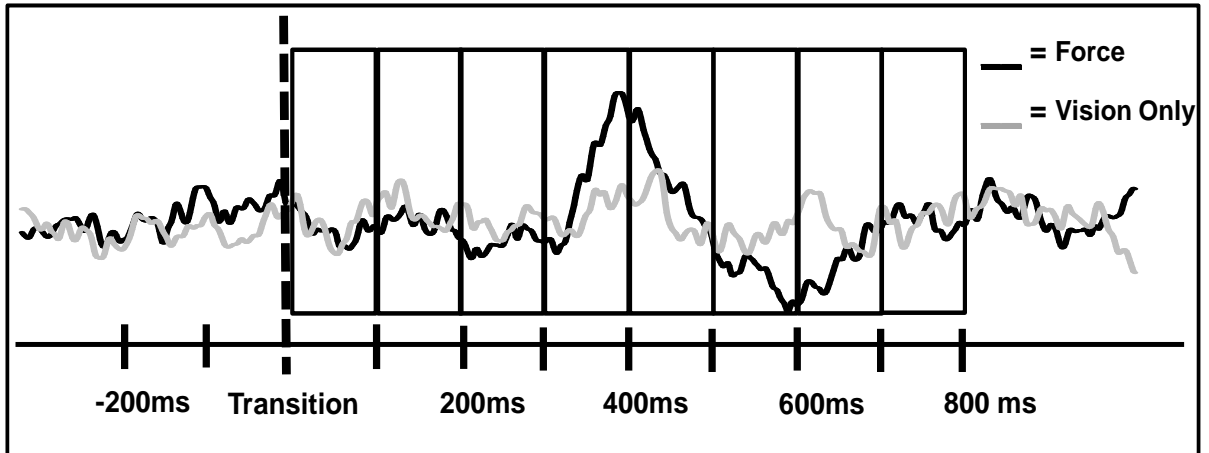


Figure 3.4. The eight 100ms time bins used to compare between vision only and force transitions in Experiment 1 and Experiment 2.

separate 2-way repeated measures ANOVA with Greenhouse-Geisser corrections (8 time bins x 2 transitions). Thirteen ROIs were selected based on standardized positions of the international 10-5 system. The ROIs covered frontal (Fpz, F3, Fz, F4), central (C3, Cz, C4), parietal (P3, Pz, P4), temporal (T7, T8), and occipital (Oz) regions. Each ROI consisted of an average cluster of 3 electrodes (Figure 1C). The two levels of transitions were examined across the eight 100ms time bins. Each significant time*transition interactions were followed with individual t-tests and corrected for multiple comparisons using Bonferroni corrections. For each interaction, a total of 8 t-tests were conducted and considered significant with a p-value < 0.00625. Electrophysiological results will be reported in terms of positive or negative polarities but no inferences will be made regarding the nature of the polarities, i.e. the structure and orientation of dipole(s) or the type of post-synaptic cells (excitatory or inhibitory).

3.3.5. Correlation analysis

To examine if there was a relationship between behavioral measures of force production and electrophysiological patterns of event-related brain activity, correlation analyses were performed using Pearson's correlation coefficient, from which we computed the coefficient of determination (r^2). The grand averaged ERP across subjects within each significant ROI was correlated with the grand averaged measure of force variability, SD. The behavioral and electrophysiological measures across each 100 ms time bins from 0 to 800 ms after changes in visual gain were plotted and best fit linear regression lines were determined for each individual ROI.

3.3.6. Source analysis

Source localization was used to understand the spatial pattern of the electrophysiological activity observed during the immediate response of the visuomotor system to gain-induced changes in visual feedback. Low-resolution electromagnetic tomographic analysis (LORETA) was applied to the difference wave obtained by subtracting the grand-averaged event-related response during the force transitions from the vision only transitions. The grand-averaged difference values, at each 100 ms time interval, that were found to be significantly different in the previous electrophysiological analysis were used to compute three-dimensional linear solutions to the inverse problem within the constraints of a realistic finite element modeling (FEM) of an average brain (EMSE® Suite). FEM is a volume-based modeling technique that considers individual anisotropic conductivities of each tissue type (skin, skull, and brain/CSF) to determine the solutions to the forward model. The distribution of neuronal generators as a current density value at each voxel and spatial resolution of 5 mm was determined. LORETA solutions are characterized with the assumption that there is highly synchronized activity among neighboring neurons and that the smoothest of all possible distributions is the most plausible to explain the data (Pascual-Marqui et al. 2002). Human Motor Area Template and prior fMRI studies from our laboratory were used to identify brain regions from the LORETA solutions (Mayka et al. 2006; Vaillancourt et al. 2003).

3.4. Results

3.4.1. Low to high visual gain: Behavioral results

The target force level across subjects ranged from 4.2-12.0 N with the mean target force = 8.44 N (SD = 2.23). The analyses examined the dependent measures in consecutive 100 ms

time bins from 0 to 800 ms after visual gain changes. Repeated measures ANOVA for mean force output was not significantly different indicating that mean force did not change across time [$F(7,70) = 2.74, p = 0.12$] (Figure 3.5A). SD of force was significantly different across time [$F(7,70) = 12.40, p = 0.0014$] (Figure 3.5B). CV of force was also significantly different across time [$F(7,70) = 14.38, p = 0.00083$] (Figure 3.5C). Tukey's HSD test subsequently detected significant increases in force variability between 300-700 ms after low to high visual gain changes. This increase in force variability by 300 ms represents the first time point when force correction was initiated by the subjects. This is consistent with previous estimates of visuomotor correction time in humans (Miall 1996). The root mean squared error (RMSE) of force production was significantly different across time [$F(9,90) = 40.628, p = 0.000032$] (Figure 3.5D). Tukey's HSD test subsequently detected a significant decrease in force error at 400 ms after gain changes. Thus, subjects were able to increase force accuracy by 400 ms following the increase in visual gain.

3.4.2. High to low visual gain: Behavioral results

The target force level across subjects ranged from 4.2-12.0 N with the mean target force = 8.25 N (SD = 2.42). The analyses examined the dependent measures in consecutive 100 ms time bins from 200 ms before to 800 ms after high-low force transition. Repeated measures ANOVA for mean force output was not significantly different indicating that mean force did not change across time [$F(7,70) = 0.50, p = 0.52$] (Figure 3.6A). SD of force was significantly different across time [$F(7,70) = 3.89, p = 0.025$] (Figure 3.6B). CV of force was also significantly different across time [$F(7,70) = 4.74, p = 0.009$] (Figure 3.6C). Tukey's HSD test subsequently detected significant increases in force variability between

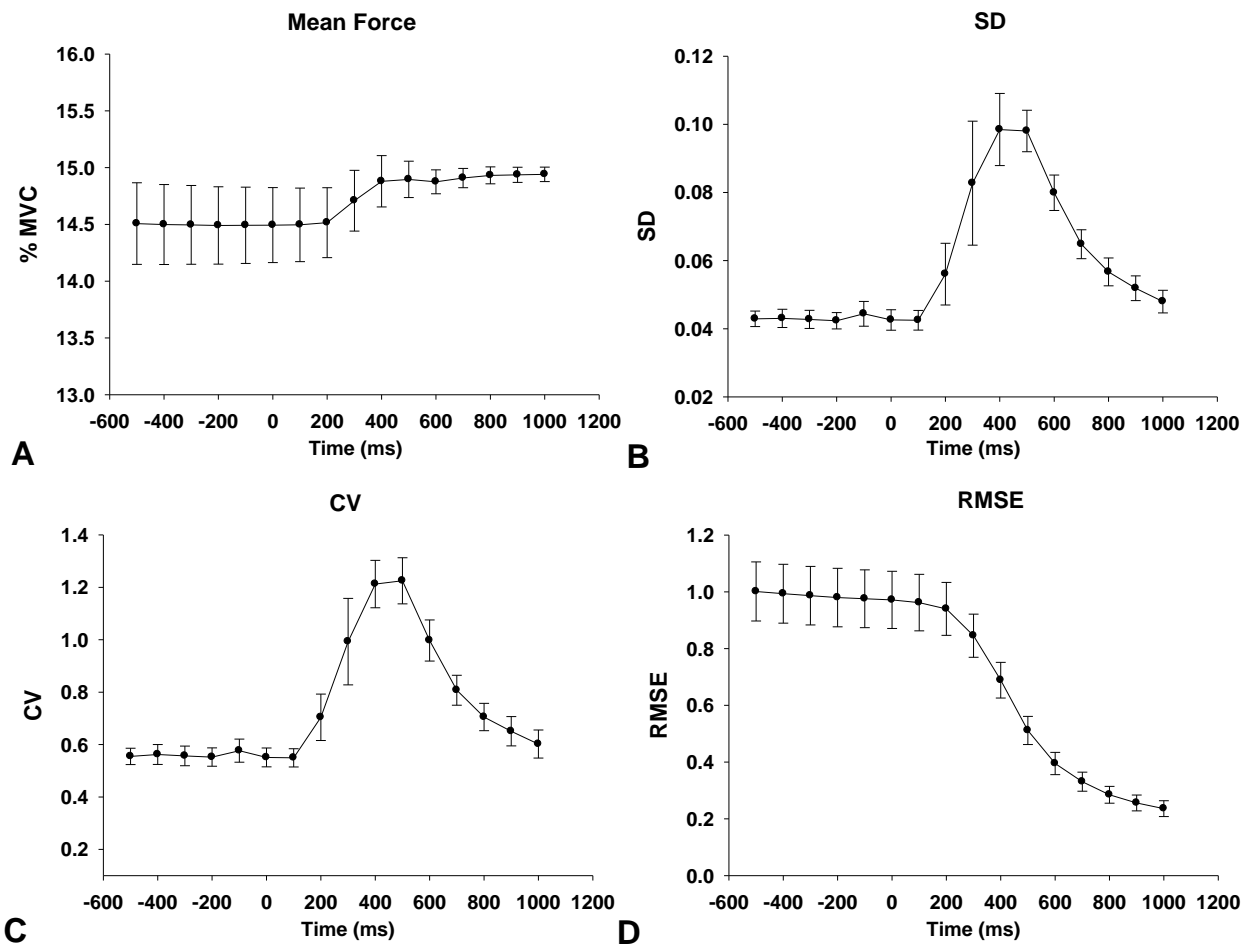


Figure 3.5. Experiment 1 behavioral data. A: Subject's mean force output before and after low to high force transition. B: Standard deviation (SD) and C: Coefficient of variation (CV) of force. D: Root mean squared error (RMSE) of force production relative to the target force following low to force gain transition.

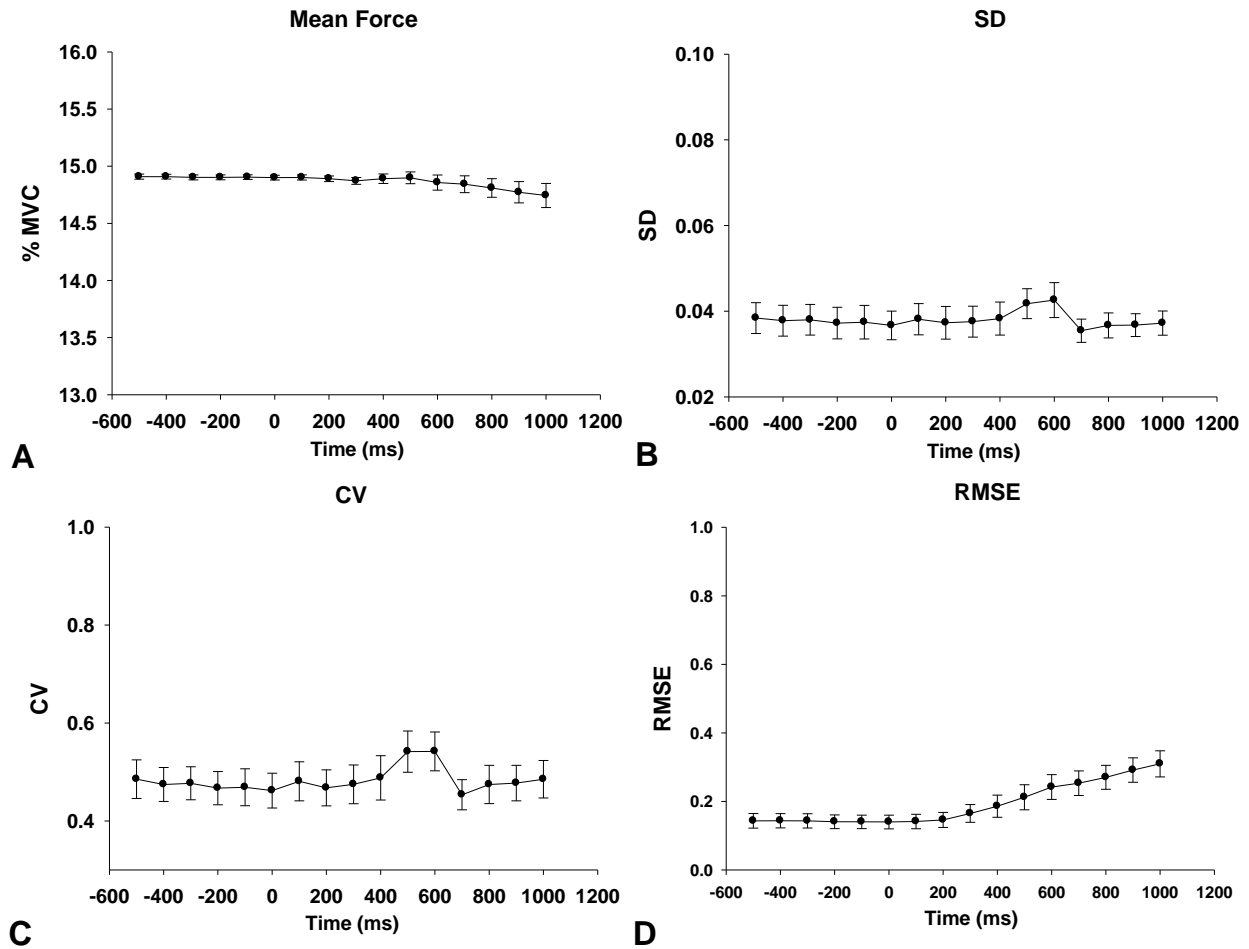


Figure 3.6. Experiment 2 behavioral data. A: Subject's mean force output before and after high to low gain transition. B: Standard deviation (SD) and C: Coefficient of variation (CV) of force. D: Root mean squared error (RMSE) of force production relative to the target force following high to low gain transition.

500 and 700 ms in the CV and 600 and 700 ms in the SD of force after high to low visual gain changes. Thus, increases in force variability occurred 200 ms earlier and to a greater extent in motor adaptation tasks involving increases in visual gain than in tasks involving decreases in visual gain. The root mean squared error (RMSE) of force production was also significantly different across time [$F(9,90) = 25.47, p = 0.000097$] (Figure 3.6D). Tukey's HSD test subsequently detected a significant increase in force error at 400 ms after changes in visual gain. Thus, subjects were able to maintain force accuracy for at least 400 ms following the decrease in visual gain.

3.4.3. Low to high visual gain: Electrophysiological results

Figure 3.7 illustrates the ERP topography map of the grand average across all 11 subjects. The potential distribution is projected onto a standardized head shape. First, a frontal-central positivity and posterior-occipital negativity was observed between 200 and 300 ms in the gain transition and to a lesser degree in the fixation transition. This was followed by a frontal negativity and parietal positivity in the gain transition between 300 and 800 ms. Significant time*transition interactions were found in 8 of the 13 ROIs (ie. Fpz, Fz, F3, F4, Pz, P3, P4, and Oz channel groups) (Table 3.1), followed by significant t-tests in 6 of the 8 significant interactions after Bonferroni corrections (i.e. Fpz, Fz, F3, F4, Pz, and P4 channel groups) (Figure 3.8). This suggests that ERPs, relating to the maintenance of force production and not the visual stimulus, were detected in these regions. Detailed results of the statistical analyses can be found in Table 2. Post-hoc t-tests revealed that significant differences occurred as early as 300 ms after the gain change. The green boxes in Figure 15 shows that the first regions with significant changes in ERPs were detected over the Fpz, F3, F4, and Pz channel groups (also see Table 3.1).

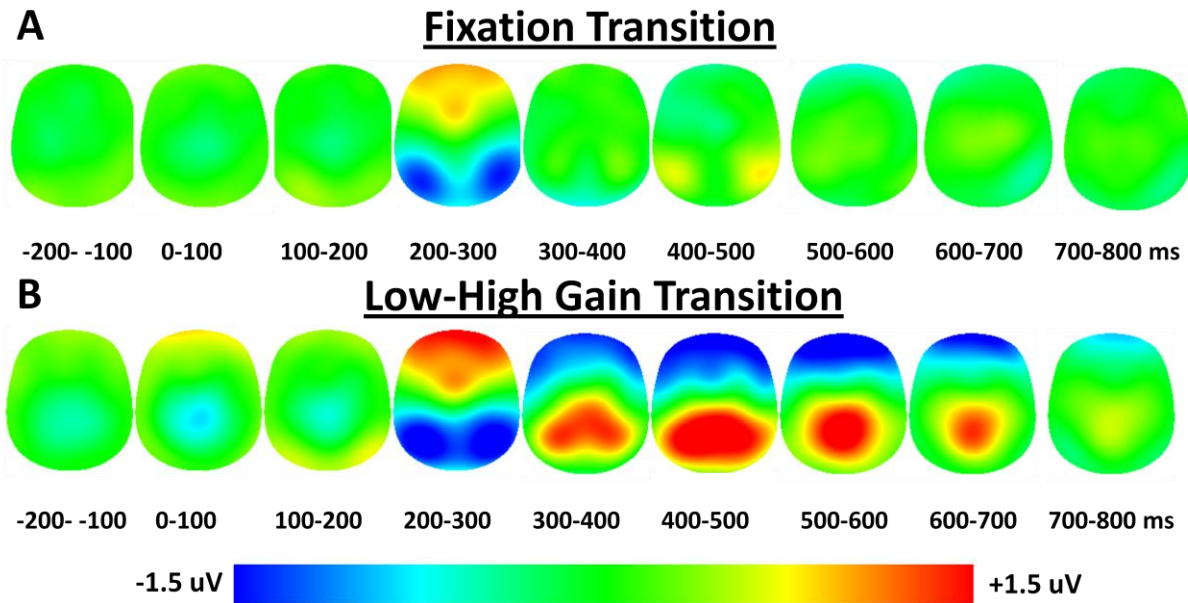


Figure 3.7. Experiment 1: Grand-average event-related topography in 100 ms time bins from -200 ms to 800 ms after (A) fixation transition and (B) low-high gain transition. The potential distribution is projected onto a standardized head shape.

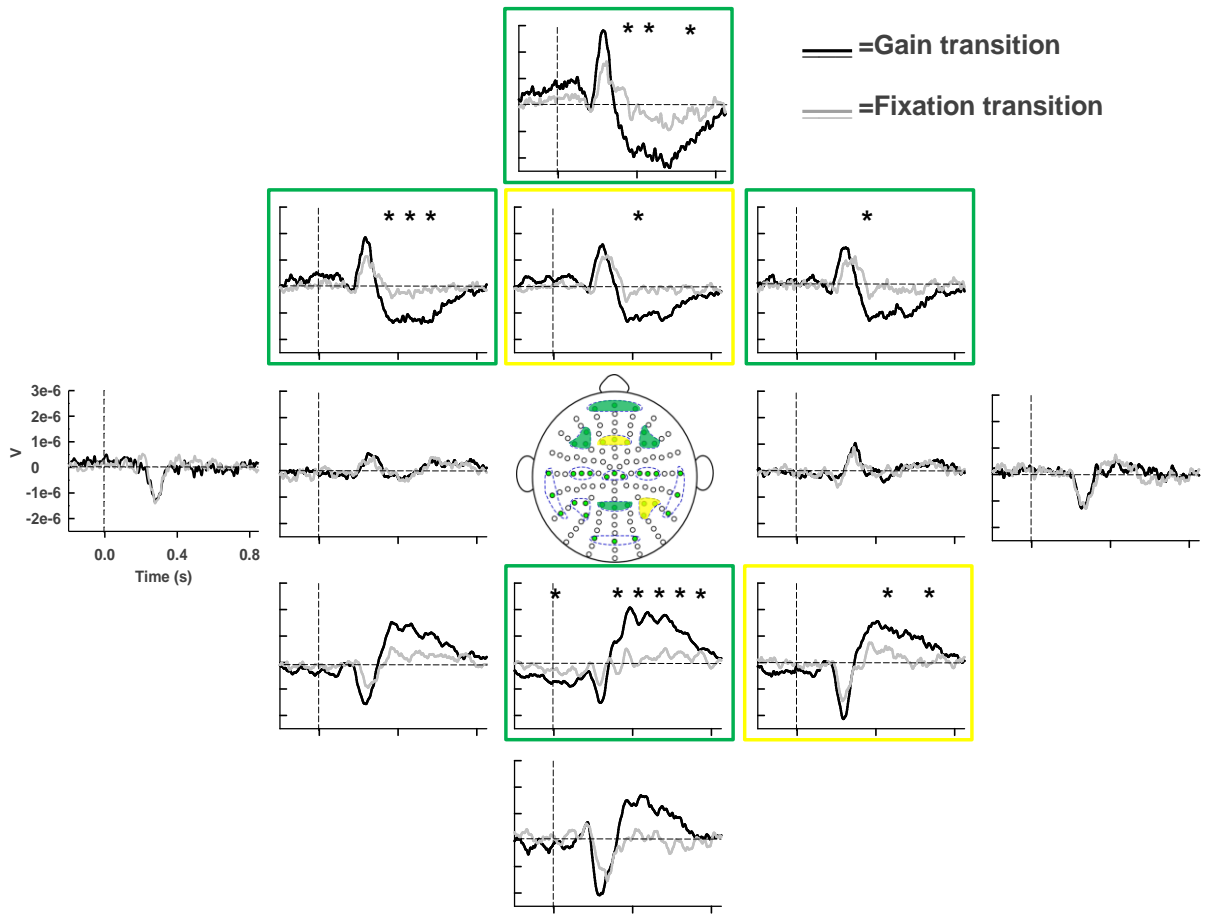


Figure 3.8. Experiment 1: Grand-average event-related potentials (ERPs) of regions of interest (ROIs) in the low-high gain transition (*black*) and fixation transition (*gray*). Statistically significant ROIs are highlighted chronologically from earliest to latest time of significance (i.e. *green* to *yellow*). * indicates significant time bins within each ROI.

Table 3 Experiment 1 ANOVA results for time*transition interaction and follow-up t-tests

Location of channel groups	F-value	Epoch (ms)		100 to 200		200-300		300 to 400		400 to 500		500 to 600		600 to 700		700 to 800		
		F(7,70)	p	t	p	t	p	t	p	t	p	t	p	t	p	t	p	
Fpz	9.71	0.001	3.40	0.01	1.80	0.10	1.74	0.11	-4.96	0.001	-3.46	0.006	-3.38	0.007	-4.14	0.002	-2.44	0.03
F3	8.94	0.0004	2.92	0.02	1.34	0.21	1.30	0.22	-3.99	0.003	-4.39	0.001	-4.28	0.002	-2.76	0.02	-1.18	0.27
Fz	5.07	0.009	2.33	0.04	0.91	0.35	1.02	0.33	-3.16	0.01	-5.62	0.0002	-2.87	0.017	-2.05	0.07	-0.95	0.36
F4	4.27	0.038	1.02	0.33	-0.14	0.89	1.22	0.25	-4.88	0.001	-3.19	0.01	-2.23	0.05	-2.27	0.05	-1.76	0.11
C3	0.36	0.800																
Cz	0.93	0.440																
C4	0.57	0.660																
P3	5.54	0.018	-1.89	0.09	-1.31	0.22	-1.44	0.18	3.19	0.01	2.99	0.01	2.78	0.02	2.76	0.02	0.71	0.49
Pz	11.81	0.0004	3.78	0.004	-1.60	0.14	-1.65	0.13	4.73	0.001	4.26	0.002	4.23	0.002	4.18	0.002	2.37	0.04
P4	7.75	0.001	-3.11	0.01	-0.58	0.58	-1.68	0.12	2.97	0.01	3.90	0.003	3.16	0.01	3.76	0.004	2.27	0.05
T7	0.47	0.750																
T8	0.69	0.620																
Oz	3.68	0.030	-1.55	0.15	-0.54	0.60	-1.15	0.28	2.34	0.04	3.29	0.01	2.61	0.03	1.98	0.08	0.85	0.42

2-way repeated measures ANOVA (8 time bins by 2 transitions) was performed. Corresponding F-values and Greenhouse-Geisser corrected p-values are shown. Each significant interaction was followed up with individual t-tests and considered significant with a Bonferroni corrected p-value < 0.00625. Corresponding t-values and p-values are shown. ROIs with significant interactions followed by significant t-tests are highlighted in bold. Significant p-values are highlighted in bold.

At 400 ms after visual feedback was removed, significant differences were found in the Fz and P4 channel groups and this is highlighted in the yellow boxes in Figure 3.8.

3.4.4. High to low visual gain: Electrophysiological results

Figure 3.9 illustrates the ERP topography map of the grand-average across all 11 subjects. The potential distribution is projected onto a standardized head shape. First, a frontal-central positivity and posterior-occipital negativity was observed between 200 and 500 ms in the gain transition. This was followed by a frontal negativity and parietal positivity in the gain transition and to a lesser degree in the fixation transition, between 500 and 800 ms.

Significant time*transition interactions were found in 5 of the 13 ROIs (i.e. Fpz, F4, Cz, Pz, and Oz channel groups) (Table 3.2), followed by significant t-tests in 3 of the 5 significant interactions after Bonferroni corrections (i.e. Fpz, Cz, and Oz channel groups) (Figure 3.10). This suggests that ERPs, relating to the maintenance of force production and not the visual stimulus, were detected in these regions. Detailed results of the statistical analyses can be found in Table 3.2. Post-hoc t-tests revealed that significant differences occurred as early as 300 ms after the gain change. The green box in Figure 3.10 shows that the first region with significant changes in ERPs was detected over the Cz channel group. At 400 ms after visual feedback was removed, significant differences were found in the Oz channel group and this is highlighted in the yellow box in Figure 3.10. Lastly, significant changes in prefrontal activity was detected from 600 to 800 ms after gain changes as shown in the red box in Figure 3.10, along with the Cz channel group, being simultaneously significant between 700 to 800 ms after gain changes.

3.4.5. Behavioral and electrophysiological correlation

Significant linear relationships were demonstrated between force variability (SD) and the event-related brain activity of ROIs in Experiment 1. Coefficient of determinations (r^2) ranged from 0.66 to 0.92, with the strongest relationship between SD and Pz. The linear functions resulted in a significant correlation at Pz ($r^2 = 0.92$, $p = 0.0002$), P4 ($r^2 = 0.70$, $p = 0.0095$), F4 ($r^2 = 0.66$, $p = 0.015$), Fz ($r^2 = 0.71$, $p = 0.0088$), F3 ($r^2 = 0.75$, $p = 0.005$), and Fpz ($r^2 = 0.79$, $p = 0.0033$). It is clear from looking at Figure 3.11A, that as force variability increases, event-related activity of parietal regions increases and event-related activity of frontal regions decreases.

In contrast to Experiment 1, there were no significant correlations found between SD and ROIs that were identified in Experiment 2 (Figure 3.11B). Coefficient of determinations (r^2) ranged from 0.003 to 0.23. The linear functions resulted in non-significant correlations at Oz ($r^2 = 0.0074$, $p = 0.84$), Cz ($r^2 = 0.003$, $p = 0.90$), and Fpz ($r^2 = 0.23$, $p = 0.22$).

3.4.6. Source estimation results

The results of the source analysis for the low to high transition can be seen in Figure 3.12 and Table 3.3. Specific brain regions corresponding to the observed solutions are overlaid onto an average brain included in the EMSE suite and distributed with the SPM (Statistical Parametric Mapping) software made available by the Wellcome Department of Imaging Neuroscience at University College London, UK. The more intense red color indicated a greater source of activation from the specific regions. The solution illustrated a strong focus of activity in the left superior parietal cortex from 300 to 500 ms after low-high force transition. Maximum current density values were identified at $X = -28$, $Y = -46$, and $Z = 50$ from 300 to 400 ms and at $X = -26$, $Y = -48$, and $Z = 50$ from 400 to 500 ms after increasing visual gain in Talairach coordinates. A strong focus of activity was also located in the right insular region from 300 to 400 ms after low-

high force transition with maximum current density values at $X=38$, $Y=12$, and $Z=7$, representing ventral premotor cortex (PMv). In addition, maximum activation from 400 to 500 ms after increasing gain was localized to bilateral dorsal premotor cortex (PMd) at $X=30$, $Y=-2$, and $Z=44$ and at $X=-18$, $Y=-9$, and $Z=52$. Maximum activation from 500 to 600 ms after increases in visual gain was localized to bilateral PMd, left PMv, and bilateral temporal cortex. Lastly, maximum activation from 600 to 700 ms was localized to the right extrastriate cortex (V3) and left anterior prefrontal cortex.

The results of the source analysis for the high to low transition can be seen in Figure 3.13 and Table 3.3. Brain regions corresponding to the observed solutions are shown with the more intense red color indicating greater source of activation from the specific regions. The solution illustrated a strong focus of activity in the right PMd and right PMv from 300 to 400 ms and right V3 from 300 to 500 ms after high-low force transition. Maximum current density values were identified at $X=54$, $Y=-9$, and $Z=24$; $X=22$, $Y=-7$, and $Z=50$; $X=28$, $Y=-78$, and $Z=-11$, from 300 to 400 ms and at $X=22$, $Y=-84$, and $Z=-6$ from 400 to 500 ms after decreasing visual gain in Talairach coordinates. Maximum activation from 600 to 700 ms after decreases in visual gain was localized to the left pre-supplementary motor area (pre-SMA) and right V3. Lastly, maximum activation from 700 to 800 ms was localized to the left pre-SMA and left temporal cortex.

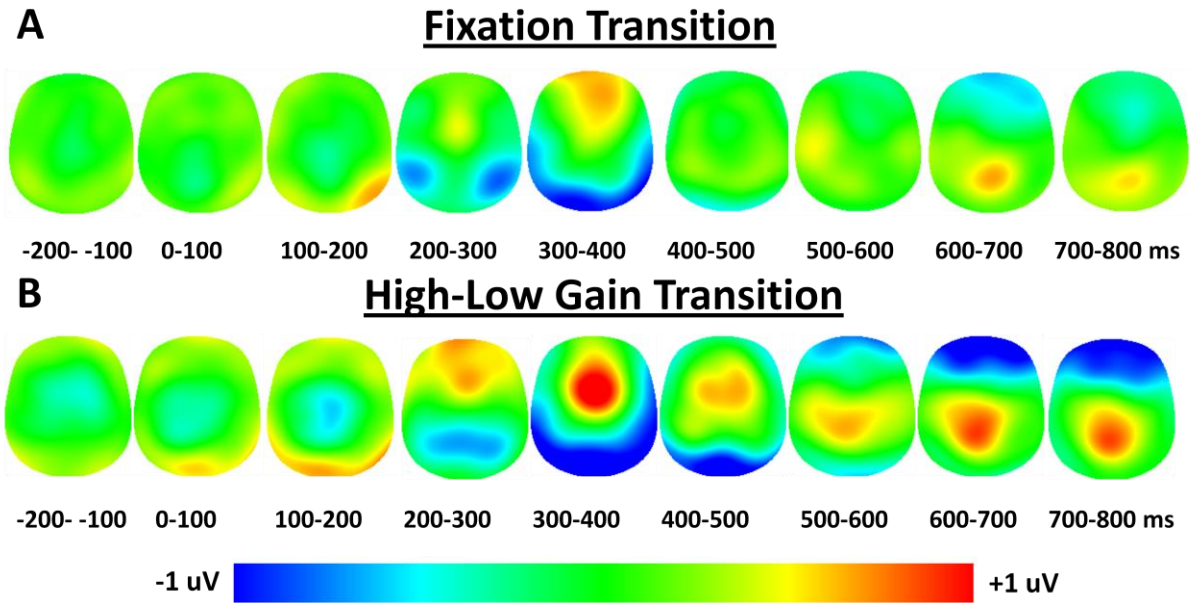


Figure 3.9. Experiment 2: Grand-average event-related topography in 100 ms time bins from -200 ms to 800 ms after (A) fixation transition and (B) high-low gain transition. The potential distribution is projected onto a standardized head shape.

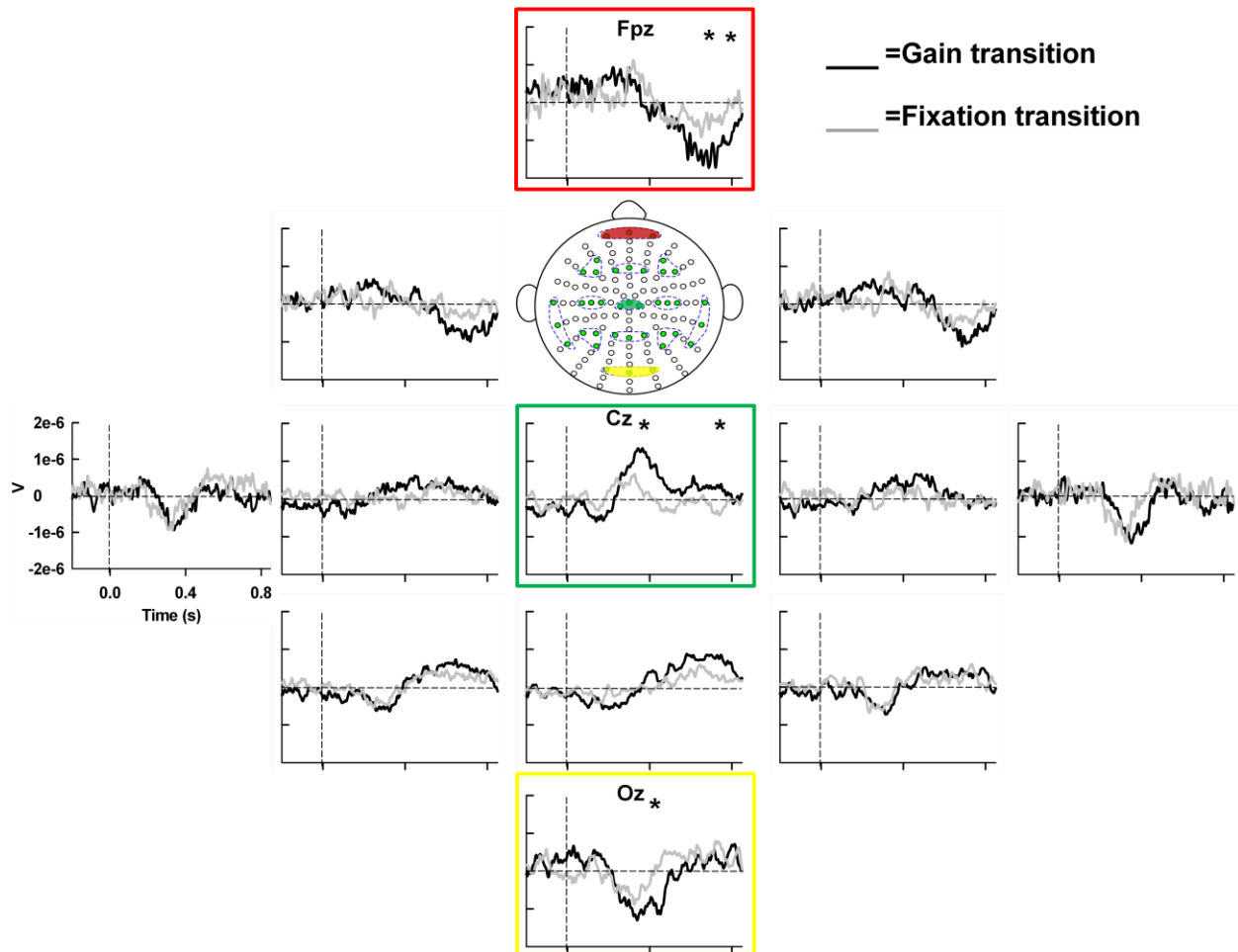


Figure 3.10. Experiment 2: Grand-average event-related potentials (ERPs) of regions of interest (ROIs) in the high-low gain transition (*black*) and fixation transition (*gray*). Statistically significant ROIs are highlighted chronologically from earliest to latest time of significance (i.e. *green* to *yellow* to *red*). * indicates significant time bins within each ROI.

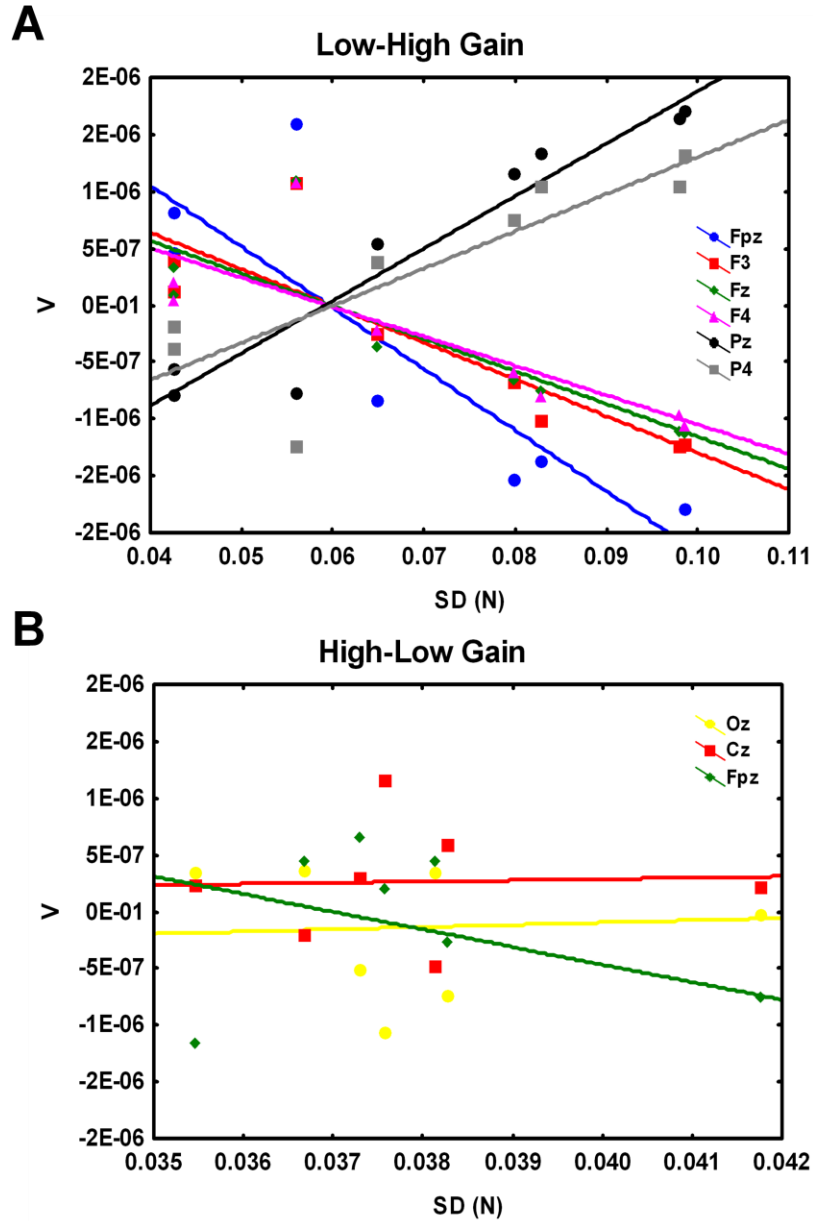


Figure 3.11. Force variability (SD) and event-related brain activity of significant ROIs in Experiment 1 (A) and Experiment 2 (B). Each data point represent the grand averaged voltage change across subjects to the force variability at each 100 ms time bin from 0 to 800 ms after force transition. The lines are the linear regression lines.

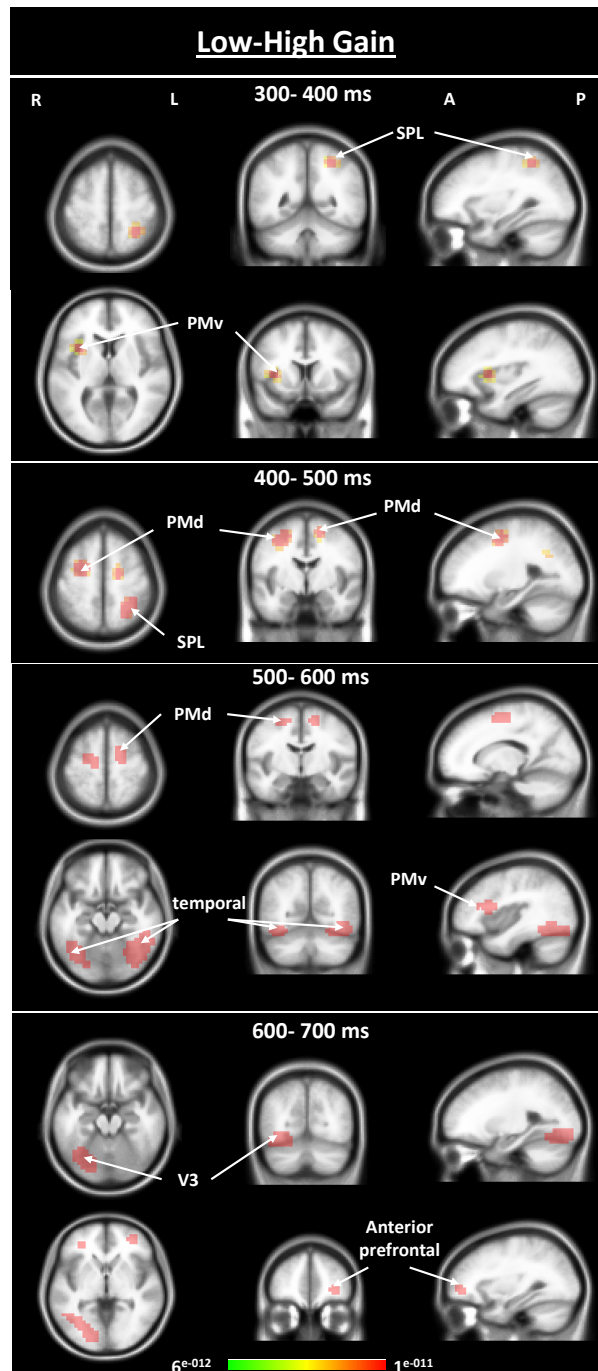


Figure 3.12. Experiment 1: Grand-averaged ERP difference results of the LORETA analysis showing current density maxima from 300 to 400 ms (top row), 400 to 500 ms (top middle row), 500 to 600 ms (bottom middle row), and 600 to 700 ms time bins (bottom row). Each map consists of axial, coronal, and sagittal slices showing the areas of maximum activation.

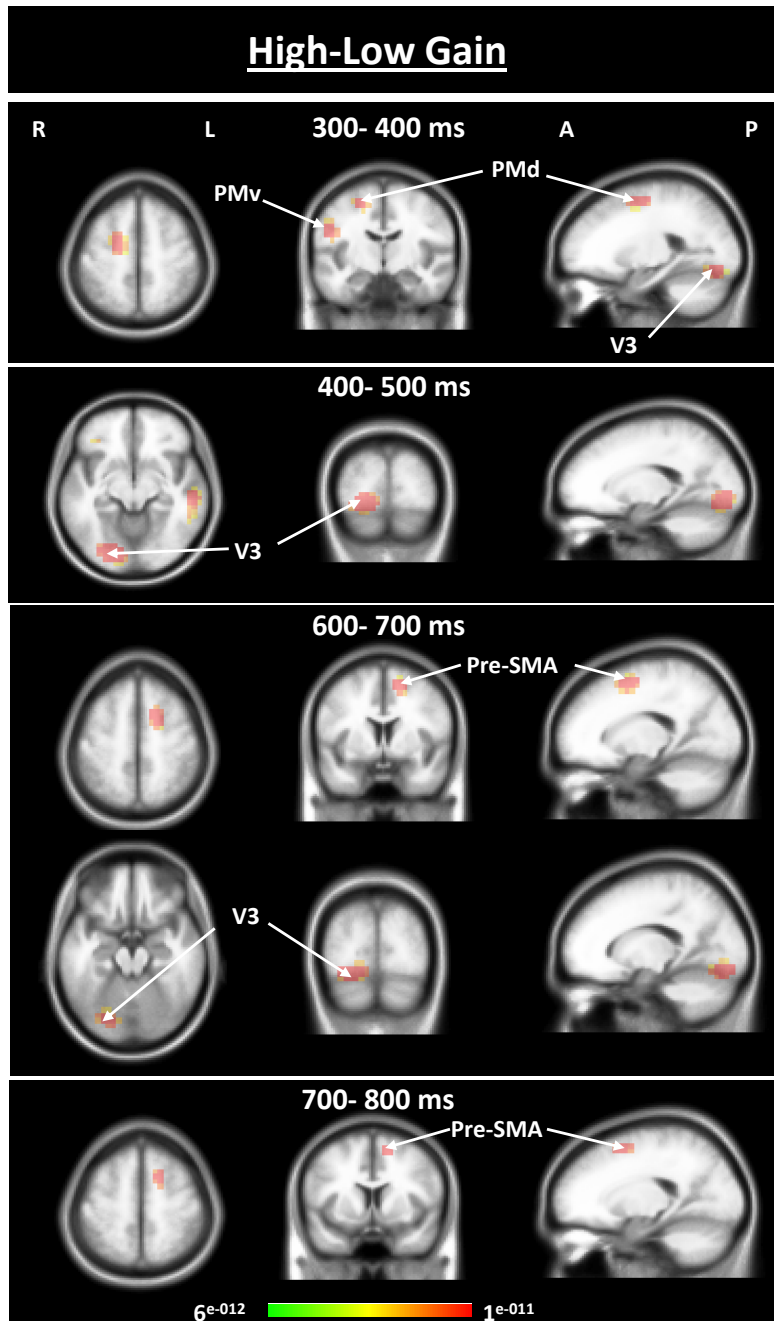


Figure 3.13. Experiment 2: Grand-averaged ERP difference results of the LORETA analysis showing current density maxima from 300 to 400 ms (top row), 400 to 500 ms (top middle row), 600 to 700 ms (bottom middle row), and 700 to 800 ms time bins (bottom row). Each map consists of axial, coronal, and sagittal slices showing the areas of maximum activation.

Table 2 Experiment 2 ANOVA results for condition by time interaction and follow-up t-tests

Location of channel	F-value	Epoch (ms)																
		0 to 100		100 to 200		200 to 300		300 to 400		400 to 500		500 to 600		600 to 700		700 to 800		
groups	F(7,70)	p	t	p	t	p	t	p	t	p	t	p	t	p	t	p		
Fpz	4.25	0.012	1.93	0.08	1.52	0.16	1.44	0.18	-1.71	0.12	-0.28	0.78	-1.46	0.18	-4.13	0.002	-3.69	0.004
F3	3.10	0.061																
Fz	2.44	0.080																
F4	3.02	0.040	-0.23	0.82	2.80	0.02	1.99	0.07	-1.49	0.17	0.69	0.51	0.44	0.67	1.59	0.14	-3.01	0.01
C3	1.72	0.185																
Cz	6.68	0.002	-1.91	0.09	-1.92	0.08	-0.54	0.60	4.47	0.001	3.41	0.007	2.65	0.02	2.35	0.04	5.29	4.E-04
C4	2.15	0.125																
T7	1.19	0.329																
P3	1.04	0.393																
Pz	4.72	0.014	-1.66	0.13	-1.18	0.26	-1.83	0.10	0.20	0.85	1.15	0.28	2.07	0.06	1.68	0.12	2.74	0.020
P4	0.75	0.492																
T8	1.09	0.350																
Oz	4.84	0.004	2.79	0.02	1.38	0.2	-0.5	0.64	-2.35	0.04	-4.12	0.002	-2.64	0.02	-1.04	0.32	-0.57	0.58

2-way repeated measures ANOVA (8 time bins by 2 transitions) was performed. Corresponding F-values and Greenhouse-Geisser corrected p-values are shown. Each significant interaction was followed up with individual t-tests and considered significant with a Bonferroni corrected p-value < 0.00625. Corresponding t-values and p-values are shown. ROIs with significant interactions followed by significant t-tests are highlighted in bold. Significant p-values are highlighted in bold.

Table 3.3 Locations of maximum activation as revealed by LORETA

Low-High	Talaraich Coordinates			High-Low	Talaraich Coordinates		
Visuomotor Area	X	Y	Z	Visuomotor Area	X	Y	Z
300-400 ms				300-400 ms			
L SPL	-28	-46	50	R PMv	54	-9	24
R PMv	38	12	7	R PMd	22	-7	50
400-500 ms				R V3	28	-78	-11
L SPL	-26	-48	50	400-500 ms			
L PMd	-18	-9	52	R V3	22	-84	-6
R PMd	30	-2	44	600-700 ms			
500-600 ms				L pre-SMA	-14	6	48
L PMd	-18	-13	54	R V3	22	-78	-11
R PMd	20	-9	56	700-800 ms			
L PMv	-40	16	12	L temporal (BA37)	-40	-58	-8
L temporal (BA37)	-40	-60	-12	L pre-SMA	-14	8	50
R temporal (BA37)	40	-60	-12				
600-700 ms							
L ant prefrontal	-30	48	-6				
R V3	36	-70	-12				

Coordinates are in standard Talaraich space.

3.5. Discussion

The central finding of this study is that adaptations to increased visual gain result in greater force variability that is systematically related to electrical activity from the fronto-parietal cortex. In contrast, a rapid decrease in visual gain did not produce the same spatiotemporal pattern of brain activity as a rapid increase in visual gain. The transition from low to high visual gain involves greater changes in parietal cortex, specifically the superior parietal cortex, than the transition from high to low visual gain. In contrast, the transition from high to low visual gain involves greater changes in occipital regions such as the right extrastriate cortex (V3) than the transition from low to high visual gain. Activity in the dorsal and ventral premotor cortices was identified during both low to high and high to low changes in visual gain.

Behavior-related correlation to event-related cortical activity

Vaillancourt and colleagues (2006a) demonstrated that force variability decreases considerably up to 1° before plateauing. Changing visual gain levels lead to changes in the spatial amplitude of visual feedback and changing the spatial amplitude of visual feedback subsequently results in a change in force output. Previous studies have consistently demonstrated a decrease in the variability of force output during static levels of high visual gain (Baweja et al. 2010; Beuter et al. 1995; Hong and Newell 2008; Stephens and Taylor 1974). However, our behavioral findings demonstrated that force variability does not improve during immediate adaptation to changes in visual gain as has been shown during static changes in visual gain. Instead, force variability increases as the visuomotor system adapts to changes in visual gain.

Our findings support the idea that event-related activity is sensitive to the immediate visuomotor error because behavioral adjustments in force production occurred very closely in

time with the detection of ERPs that resemble both error-related negativity (ERN or Ne) and error-related positivity (Pe), often linked to evaluation processes and error monitoring, respectively (Coles et al. 1995; Falkenstein et al. 1991; Falkenstein et al. 2000). The sustained event-related pattern observed during increases in visual gain covers a wide range of frontal and parietal regions that resemble error-related activity observed during sensorimotor adaptation tasks (Anguera et al. 2009; Falkenstein et al. 2000; Krigolson and Holroyd 2006). Changes in force variability and Ne/Pe components were both detected by 300 ms after increases in visual gain. A study by Anguera and colleagues (2009) was able to show a positive scaling of ERN amplitudes to error magnitude during a sensorimotor adaptation task. The prominent Ne and Pe components after increases in visual gain may therefore reflect the correction of error during force production.

In addition, results from the behavioral and electrocortical correlation analysis after increases in visual gain provide support to the idea that changes in the magnitude of isometric force variability is related to the inherent properties of event-related brain activity. As force variability increases, event-related activity of parietal regions increases while event-related activity of frontal regions decreases (Figure 3.11A). The strongest correlation was found at the midline parietal area (Pz) and this region was also identified through source analysis as one of the brain region primarily responsible for the observed event-related activity between 300 and 400 ms after increases in visual gain. This relationship is evident during immediate increases in visual gain when force variability changes to a significantly greater degree than during decreases in visual gain (Figures 3.5 and 3.6). A possible explanation as to why no such relationship between force variability and brain activity were observed during decreases in visual gain could be due to the smaller degree of behavioral change that occurred after decreases in visual

feedback relative to the increased force variability induced after immediate increases in visual feedback.

Regions involved with immediate increases in visual gain

A novel finding with increasing visual gain is that event-related activities were observed across frontal and parietal regions as early as 300 ms (Fpz, F3, F4, and Pz channel groups) and 400 ms (Fz and P4) after increases in the visual gain. Cortical localization (LORETA) indicated left SPL and right PMv as the brain regions primarily responsible for the observed event-related activity between 300 and 400 ms (Figure 3.12). Next, the left SPL and bilateral PMd were identified between 400 and 500 ms. Both electrophysiological and tomographical analyses suggest that subjects rely on a visuomotor system involving frontal and parietal regions during the immediate transition from a low to high spatial gain of visual feedback. The human anterior IPS (hAIP), which is generally believed to be part of the SPL, is a region that has been linked with visually-guided grasping (Binkofski et al. 1998; Castiello 2005; Culham et al. 2006). Several studies have demonstrated the importance of AIP in grip force scaling through TMS-induced inactivations of the AIP (Dafotakis et al. 2008; Davare et al. 2007; Tunik et al. 2005). Based on their findings, they concluded that AIP contributes to the detection and correction of errors in grip force scaling. Our behavioral finding of significant differences in force variability by 300 ms, along with source localization to the AIP between 300 and 500 ms, compliments earlier evidence that the AIP plays an important role during grip force error. Our findings extend this notion to tasks involving immediate increases in visual gain.

Regions involved with immediate decreases in visual gain

A novel finding with decreases in visual gain is that the first significant event-related activities occurred as early as 300 ms in the midline central region (Cz channel group) and 400 ms in the midline occipital region (Oz channel group) after a sudden decrease in visual gain. Cortical localization (LORETA) indicated right PMd, right PMv, and right V3 as the brain regions primarily responsible for the observed event-related activity between 300 and 400 ms after a decrease in visual gain (Figure 3.13). Therefore, both electrophysiological and tomographical analysis support the findings that subjects rely on a visuomotor system involving frontal and occipital regions during the immediate transitions from high to low spatial gain of visual feedback. The extrastriate visual area V3 was identified as one of the regions primarily responsible for the observed event-related activity between 300 and 700 ms after the decrease in visual gain. This finding complements evidence from an fMRI study that demonstrated BOLD response changes within the extrastriate visual cortex, specifically V3 and V5, during static low visual gain levels (Coombes et al. 2010a). This finding also shows that the occipital region is sensitive to immediate decreases in the spatial amplitude of visual feedback. This is in agreement with previously identified involvement of extrastriate visual area MT (that is homologous to V5 in humans) with the processing of the spatial properties of visual feedback (Ungerleider and Haxby 1994; Ungerleider and Mishkin 1982). Together, these findings suggest that the extrastriate visual cortex, specifically V3, contributes to the maintenance of force production during immediate decreases in visual gain.

Common regions involved with immediate changes in visual gain

A study by Mizelle and colleagues (2010) observed greater EEG oscillatory activity in the parietal regions during lower extremity tasks that required greater visual demands than proprioceptive demands. Premotor regions, on the other hand, were shown to be most sensitive

during higher proprioceptive demands. Results from our study compliments Mizelle's study because we similarly detected greater activity in parietal regions during a task requiring greater visual demands because of the increase in visual feedback gain. The localization of premotor and parietal regions during increases in visual gain is consistent with previous evidence identifying connections between SPL and PMd during visuomotor tasks in non-human primates (Binkofski et al. 1999; Caminiti et al. 1996; Wise et al. 1997). The current findings extend previous knowledge to a greater involvement of a premotor-parietal network during immediate increases in visual gain than during decreases in visual gain. In addition, premotor regions were identified during both increases and decreases in visual gain and this finding is consistent with a prior fMRI study which identified premotor activity during both low and high static levels of visual gain (Coombes et al. 2010a). This observation could also be explained by the similar attention to proprioceptive demands required during both tasks in maintaining accurate precision grip force production (Mizelle et al. 2010). The premotor cortex has also been associated with multisensory integration (Graziano et al. 1997; Rizzolatti et al. 1981). In the present study, subjects performed a motor task using a combination of sensory information (i.e. visual and proprioceptive), therefore it is possible that the measured premotor responses reflect enhanced sensorimotor integration mechanisms.

Summary

A differential visuomotor network is involved during immediate changes in visual gain, with activity localized in left SPL, bilateral PMv, and bilateral PMd after immediate increases in visual gain. On the other hand, localized activity was identified in the right V3, right PMv, and right PMd after immediate decreases in visual gain. Together, these findings suggest that the

visuomotor areas of PMd and PMv contribute to the overall maintenance of force production during immediate changes in visual gain. However, our results suggest an increased reliance on SPL during tasks involving a greater amount of visual feedback. Importantly, the increase in visual gain triggered increased force variability that was highly correlated with the event-related electrocortical activity in parietal-frontal circuits.

CHAPTER 4

CONCLUSIONS

Three different EEG experiments were conducted to investigate the dynamic spatiotemporal patterns of brain activity during precision grip force in healthy individuals. The first study used EEG to investigate the cortical regions that are involved when healthy individuals transition from producing visually guided to memory guided precision grip force contractions. The second study, consisting of two experiments, used EEG to investigate the cortical regions involved when healthy individuals adapt to immediate changes in visual gain i.e. increasing and decreasing visual gains. The following sections discuss conclusions for each of these experiments and possible directions for future work.

4.1. Chapter 2 Conclusions

It is well established that the prefrontal cortex is involved during memory guided tasks whereas visually guided tasks are controlled in part by a frontal-parietal network. However, the dynamic nature of the transition from visually guided to memory guided force control is not as well established. As such, the experiment in Chapter 2 examined the spatiotemporal pattern of brain activity that occurs during the immediate transition from visually guided to memory guided force control. After visual feedback was removed, the first significant change in event-related activity occurred in the contralateral central region (C3), followed by changes in prefrontal cortex (Fpz). Low-resolution electromagnetic tomography (LORETA) localized maximum activity to the left ventral premotor cortex and right ventral prefrontal cortex. The findings showed that subjects rely on sensorimotor memory processes involving left ventral premotor cortex and right ventral prefrontal cortex after the immediate transition from visually guided to

memory guided force control. Since the premotor cortex and prefrontal cortex are affected by both aging and by specific neurological disorders, an area of future research would be to conduct subsequent EEG studies that investigate the brain mechanisms that underlie memory-guided motor output in healthy aging and in disease. Another possible application for this work is to target identified brain regions during stimulation therapy to assist with neuroplasticity.

4.2. Chapter 3 Conclusions

When the spatial amplitude of visual feedback is increased through manipulating visual gain, motor performance improves as measured by reduced force output variability. Specific brain regions of the visuomotor system have been shown to respond selectively to different static levels of visual gain. In many instances, however, humans are required to adapt to acute changes in visual information, and how force variability and activity within parietal-frontal circuits respond during adaptations to visual gain remains less clear. As such, the experiments in Chapter 3 examined the spatiotemporal pattern of brain activity during the immediate adaptation to changes in visual gain. The transition consisted of going from low to high visual gain and high to low visual gain. The findings showed that adaptations to increased visual gain resulted in greater force variability that related to electrical activity from the fronto-parietal cortex. In contrast, a rapid decrease in visual gain did not produce the same spatiotemporal pattern of brain activity as a rapid increase in visual gain. The transition from low to high visual gain involved greater changes in the parietal cortex, specifically the superior parietal cortex, while the transition from high to low visual gain involved greater changes in occipital regions such as the right extrastriate cortex (V3). Activity in the dorsal and ventral premotor cortices was identified during both low to high and high to low changes in visual gain. Our results suggest that increased

visual gain triggered increased force variability that was related to electrocortical activity in parietal-frontal circuits. An interesting area of future work would be to examine the transition across different force levels and determining if the relationship between electrocortical activity and force behavior is dependent on the relative amount of force exerted by the subjects.

CITED LITERATURE

- Anguera JA, Seidler RD, and Gehring WJ.** Changes in performance monitoring during sensorimotor adaptation. *J Neurophysiol* 102: 1868-1879, 2009.
- Baker S, Frith C, Frackowiak R, and Dolan R.** Active representation of shape and spatial location in man. *Cerebral Cortex* 6: 612-619, 1996.
- Barbey AK, Koenigs M, and Grafman J.** Orbitofrontal contributions to human working memory. *Cereb Cortex* 21: 789-795, 2011.
- Baweja HS, Kennedy DM, Vu J, Vaillancourt DE, and Christou EA.** Greater amount of visual feedback decreases force variability by reducing force oscillations from 0-1 and 3-7 Hz. *Eur J Appl Physiol* 108: 935-943, 2010.
- Bender S, Behringer S, Freitag CM, Resch F, and Weisbrod M.** Transmodal comparison of auditory, motor, and visual post-processing with and without intentional short-term memory maintenance. *Clin Neurophysiol* 121: 2044-2064, 2010.
- Beuter A, Haverkamp H, Glass L, and Carrière L.** Effect of manipulating visual feedback parameters on eye and finger movements. *Int J Neurosci* 83: 281-294, 1995.
- Binkofski F, Buccino G, Posse S, Seitz RJ, Rizzolatti G, and Freund H.** A fronto-parietal circuit for object manipulation in man: evidence from an fMRI-study. *Eur J Neurosci* 11: 3276-3286, 1999.
- Binkofski F, Dohle C, Posse S, Stephan KM, Hefter H, Seitz RJ, and Freund HJ.** Human anterior intraparietal area subserves prehension: a combined lesion and functional MRI activation study. *Neurology* 50: 1253-1259, 1998.
- Binsted G, Rolheiser TM, and Chua R.** Decay in visuomotor representations during manual aiming. *J Mot Behav* 38: 82-87, 2006.
- Brass M, Ullsperger M, Knoesche TR, von Cramon DY, and Phillips NA.** Who comes first? The role of the prefrontal and parietal cortex in cognitive control. *J Cogn Neurosci* 17: 1367-1375, 2005.
- Brignani D, Bortoletto M, Miniussi C, and Maioli C.** The when and where of spatial storage in memory-guided saccades. *Neuroimage* 52: 1611-1620, 2010.
- Bunge SA, Hazeltine E, Scanlon MD, Rosen AC, and Gabrieli JD.** Dissociable contributions of prefrontal and parietal cortices to response selection. *Neuroimage* 17: 1562-1571, 2002.
- Caminiti R, Ferraina S, and Johnson P.** The sources of visual information to the primate frontal lobe: a novel role for the superior parietal lobule. *Cereb Cortex* 6: 319-328, 1996.
- Caminiti R, Johnson P, Galli C, Ferraina S, and Burnod Y.** Making arm movements within different parts of space: the premotor and motor cortical representation of a coordinate system for reaching to visual targets. *J Neurosci* 11: 1182-1197, 1991.
- Carlton L.** Processing visual feedback information for movement control. *J Exp Psychol Hum Percept Perform* 7: 1019-1030, 1981.
- Castiello U.** The neuroscience of grasping. *Nat Rev Neurosci* 6: 726-736, 2005.
- Chafee MV, and Goldman-Rakic PS.** Inactivation of parietal and prefrontal cortex reveals interdependence of neural activity during memory-guided saccades. *J Neurophysiol* 83: 1550-1566, 2000.
- Cohen JD, Perlstein WM, Braver TS, Nystrom LE, Noll DC, Jonides J, and Smith EE.** Temporal dynamics of brain activation during a working memory task. *Nature* 386: 604-608, 1997.

Coles MG, Scheffers MK, and Fournier L. Where did you go wrong? Errors, partial errors, and the nature of human information processing. *Acta Psychol (Amst)* 90: 129-144, 1995.

Coombes S, Corcos D, Sprute L, and Vaillancourt D. Selective Regions of the Visuomotor System Are Related to Gain-Induced Changes in Force Error. *Journal of Neurophysiology* 2114-2123, 2010a.

Coombes S, Corcos D, and Vaillancourt D. Spatiotemporal tuning of brain activity and force performance. *Neuroimage* In Press, 2010b.

Culham J, Cavina-Pratesi C, and Singhal A. The role of parietal cortex in visuomotor control: what have we learned from neuroimaging? *Neuropsychologia* 44: 2668-2684, 2006.

Curtis CE, and D'Esposito M. Persistent activity in the prefrontal cortex during working memory. *Trends in Cognitive Sciences* 7: 415-423, 2003.

Curtis CE, and D'Esposito M. The effects of prefrontal lesions on working memory performance and theory. *Cogn Affect Behav Neurosci* 4: 528-539, 2004.

D'Esposito M, Aguirre G, Zarahn E, Ballard D, Shin R, and Lease J. Functional MRI studies of spatial and nonspatial working memory. *Cognitive Brain Research* 7: 1-13, 1998.

Dafotakis M, Sparing R, Eickhoff SB, Fink GR, and Nowak DA. On the role of the ventral premotor cortex and anterior intraparietal area for predictive and reactive scaling of grip force. *Brain Res* 1228: 73-80, 2008.

Davare M, Andres M, Clerget E, Thonnard JL, and Olivier E. Temporal dissociation between hand shaping and grip force scaling in the anterior intraparietal area. *J Neurosci* 27: 3974-3980, 2007.

Dawson G. Cerebral Responses to Electrical Stimulation of Peripheral Nerve in Man. *J Neurol Neurosurg Psychiatry*: 1947, p. 134-140.

Debaere F, Wenderoth N, Sunaert S, Van Hecke P, and Swinnen SP. Internal vs external generation of movements: differential neural pathways involved in bimanual coordination performed in the presence or absence of augmented visual feedback. *Neuroimage* 19: 764-776, 2003.

Donchin E. Presidential address, 1980. Surprise!...Surprise? *Psychophysiology* 18: 493-513, 1981.

Ehrsson HH, Fagergren E, and Forsberg H. Differential fronto-parietal activation depending on force used in a precision grip task: an fMRI study. *J Neurophysiol* 85: 2613-2623, 2001.

Elliott D, and Madalena J. The influence of premovement visual information on manual aiming. *Q J Exp Psychol A* 39: 541-559, 1987.

Falkenstein M, Hohnsbein J, Hoormann J, and Blanke L. Effects of crossmodal divided attention on late ERP components. II. Error processing in choice reaction tasks. *Electroencephalogr Clin Neurophysiol* 78: 447-455, 1991.

Falkenstein M, Hoormann J, Christ S, and Hohnsbein J. ERP components on reaction errors and their functional significance: a tutorial. *Biol Psychol* 51: 87-107, 2000.

Fell J, Dietl T, Grunwald T, Kurthen M, Klaver P, Trautner P, Schaller C, Elger C, and Fernández G. Neural bases of cognitive ERPs: more than phase reset. *J Cogn Neurosci* 16: 1595-1604, 2004.

Fuster JM. Unit activity in prefrontal cortex during delayed-response performance: neuronal correlates of transient memory. *J Neurophysiol* 36: 61-78, 1973.

Fuster JM, and Alexander GE. Neuron activity related to short-term memory. *Science* 173: 652-654, 1971.

- Gallace A, and Spence C.** The cognitive and neural correlates of tactile memory. *Psychol Bull* 135: 380-406, 2009.
- Gentili RJ, Bradberry TJ, Oh H, Hatfield BD, and Vidal JL.** Cerebral cortical dynamics during visuomotor transformation: adaptation to a cognitive-motor executive challenge. *Psychophysiology* 48: 813-824, 2011.
- Glickstein M.** How are visual areas of the brain connected to motor areas for the sensory guidance of movement? *Trends in Neurosciences* 23: 613-617, 2000.
- Goldman-Rakic PS.** Topography of cognition: parallel distributed networks in primate association cortex. *Annu Rev Neurosci* 11: 137-156, 1988.
- Graziano MS, Hu XT, and Gross CG.** Visuospatial properties of ventral premotor cortex. *J Neurophysiol* 77: 2268-2292, 1997.
- Grea H, Pisella L, Rossetti Y, Desmurget M, Tilikete C, Grafton S, Prablanc C, and Vighetto A.** A lesion of the posterior parietal cortex disrupts on-line adjustments during aiming movements. *Neuropsychologia* 40: 2471-2480, 2002.
- Grol MJ, Majdandžić J, Stephan KE, Verhagen L, Dijkerman HC, Bekkering H, Verstraten FA, and Toni I.** Parieto-frontal connectivity during visually guided grasping. *J Neurosci* 27: 11877-11887, 2007.
- Hamidi M, Tononi G, and Postle BR.** Evaluating the role of prefrontal and parietal cortices in memory-guided response with repetitive transcranial magnetic stimulation. *Neuropsychologia* 47: 295-302, 2009.
- Hong S, and Newell K.** Visual information gain and the regulation of constant force levels. *Experimental Brain Research* 189: 61-69, 2008.
- Inoue M, Mikami A, Ando I, and Tsukada H.** Functional brain mapping of the macaque related to spatial working memory as revealed by PET. *Cereb Cortex* 14: 106-119, 2004.
- Jahanshahi M, Jenkins I, Brown R, Marsden C, Passingham R, and Brooks D.** Self-initiated versus externally triggered movements. I. An investigation using measurement of regional cerebral blood flow with PET and movement-related potentials in normal and Parkinson's disease subjects. *Brain* 118 (Pt 4): 913-933, 1995.
- Jeannerod M, Arbib M, Rizzolatti G, and Sakata H.** Grasping objects: the cortical mechanisms of visuomotor transformation. *Trends Neurosci* 18: 314-320, 1995.
- Jenkins IH, Jahanshahi M, Jueptner M, Passingham RE, and Brooks DJ.** Self-initiated versus externally triggered movements. II. The effect of movement predictability on regional cerebral blood flow. *Brain* 123 (Pt 6): 1216-1228, 2000.
- Johnson PB, Ferraina S, Bianchi L, and Caminiti R.** Cortical networks for visual reaching: Physiological and anatomical organization of frontal and parietal lobe arm regions. *Cerebral Cortex* 6: 102-119, 1996.
- Johnston J, Rearick M, and Slobounov S.** Movement-related cortical potentials associated with progressive muscle fatigue in a grasping task. *Clin Neurophysiol* 112: 68-77, 2001.
- Jonides J, Smith E, Koeppe R, Awh E, Minoshima S, and Mintun M.** Spatial Working-Memory in Humans as Revealed by PET. *Nature* 363: 623-625, 1993.
- Kawashima R, Okuda J, Umetsu A, Sugiura M, Inoue K, Suzuki K, Tabuchi M, Tsukiura T, Narayan SL, Nagasaka T, Yanagawa I, Fujii T, Takahashi S, Fukuda H, and Yamadori A.** Human cerebellum plays an important role in memory-timed finger movement: An fMRI study. *Journal of Neurophysiology* 83: 1079-1087, 2000.
- Keele S, and Posner M.** Processing of visual feedback in rapid movements. *J Exp Psychol* 77: 155-158, 1968.

Krakauer JW, Ghilardi MF, Mentis M, Barnes A, Veytsman M, Eidelberg D, and Ghez C. Differential cortical and subcortical activations in learning rotations and gains for reaching: A PET study. *Journal of Neurophysiology* 91: 924-933, 2004a.

Krakauer JW, Ghilardi MF, Mentis M, Barnes A, Veytsman M, Eidelberg D, and Ghez C. Differential cortical and subcortical activations in learning rotations and gains for reaching: a PET study. *Journal of Neurophysiology* 91: 924-933, 2004b.

Krigolson OE, and Holroyd CB. Evidence for hierarchical error processing in the human brain. *Neuroscience* 137: 13-17, 2006.

Kubota K, and Niki H. Prefrontal cortical unit activity and delayed alternation performance in monkeys. *J Neurophysiol* 34: 337-347, 1971.

Kuhtz-Buschbeck JP, Ehrsson HH, and Forssberg H. Human brain activity in the control of fine static precision grip forces: an fMRI study. *Eur J Neurosci* 14: 382-390, 2001.

Lang W, Starr A, Lang V, Lindinger G, and Deecke L. Cortical DC potential shifts accompanying auditory and visual short-term memory. *Electroencephalogr Clin Neurophysiol* 82: 285-295, 1992.

Makeig S, Westerfield M, Jung TP, Enghoff S, Townsend J, Courchesne E, and Sejnowski TJ. Dynamic brain sources of visual evoked responses. *Science* 295: 690-694, 2002.

Mayka M, Corcos D, Leurgans S, and Vaillancourt D. Three-dimensional locations and boundaries of motor and premotor cortices as defined by functional brain imaging: a meta-analysis. *Neuroimage* 31: 1453-1474, 2006.

McCarthy G, Puce A, Constable RT, Krystal JH, Gore JC, and Goldman-Rakic P. Activation of human prefrontal cortex during spatial and nonspatial working memory tasks measured by functional MRI. *Cereb Cortex* 6: 600-611, 1996.

Mecklinger A, Gruenewald C, Besson M, Magnie M, and Von Cramon D. Separable neuronal circuitries for manipulable and non-manipulable objects in working memory. *Cerebral Cortex* 12: 1115-1123, 2002.

Mecklinger A, Gruenewald C, Weiskopf N, and Doeller C. Motor affordance and its role for visual working memory: Evidence from fMRI studies. *Experimental Psychology* 51: 258-269, 2004.

Mecklinger A, and Pfeifer E. Event-related potentials reveal topographical and temporal distinct neuronal activation patterns for spatial and object working memory. *Brain Res Cogn Brain Res* 4: 211-224, 1996.

Meunier M, Bachevalier J, and Mishkin M. Effects of orbital frontal and anterior cingulate lesions on object and spatial memory in rhesus monkeys. *Neuropsychologia* 35: 999-1015, 1997.

Miall RC, Reckess GZ, and Imamizu H. The cerebellum coordinates eye and hand tracking movements. *Nature Neuroscience* 4: 638-644, 2001.

Michel C, Murray M, Lantz G, Gonzalez S, Spinelli L, and de Peralta R. EEG source imaging. *Clinical Neurophysiology* 115: 2195-2222, 2004.

Middleton FA, and Strick PL. Cerebellar output: motor and cognitive channels. *Trends in Cognitive Sciences* 2: 348-354, 1998.

Miller EK, Erickson CA, and Desimone R. Neural mechanisms of visual working memory in prefrontal cortex of the macaque. *J Neurosci* 16: 5154-5167, 1996.

Mishkin M, Lewis M, and Ungerleider L. Equivalence of parieto-preoccipital subareas for visuospatial ability in monkeys. *Behav Brain Res* 6: 41-55, 1982.

Mizelle JC, Forrester L, Hallett M, and Wheaton LA. Electroencephalographic reactivity to unimodal and bimodal visual and proprioceptive demands in sensorimotor integration. *Exp Brain Res* 203: 659-670, 2010.

Mottaghy FM, Gangitano M, Sparing R, Krause BJ, and Pascual-Leone A. Segregation of areas related to visual working memory in the prefrontal cortex revealed by rTMS. *Cereb Cortex* 12: 369-375, 2002.

Mueller VA, Brass M, Waszak F, and Prinz W. The role of the preSMA and the rostral cingulate zone in internally selected actions. *Neuroimage* 37: 1354-1361, 2007.

Mushiake H, Inase M, and Tanji J. Neuronal-activity in the primate premotor, supplementary, and precentral motor cortex during visually guided and internally determined sequential movements. *Journal of Neurophysiology* 66: 705-718, 1991.

Müller NG, and Knight RT. The functional neuroanatomy of working memory: contributions of human brain lesion studies. *Neuroscience* 139: 51-58, 2006.

Newell K, and McDonald P. Information, Coordination Modes and Control in a Prehensile Force Task. *Human Movement Science* 13: 375-391, 1994a.

Newell KM, and McDonald PV. Information, Coordination Modes, and Control in a Prehensile Force Task. *Human Movement Science* 13: 375-391, 1994b.

Nieder A, and Miller EK. A parieto-frontal network for visual numerical information in the monkey. *Proc Natl Acad Sci U S A* 101: 7457-7462, 2004.

Oliveri M, Turriziani P, Carlesimo GA, Koch G, Tomaiuolo F, Panella M, and Caltagirone C. Parieto-frontal interactions in visual-object and visual-spatial working memory: evidence from transcranial magnetic stimulation. *Cereb Cortex* 11: 606-618, 2001.

Oostenveld R, and Praamstra P. The five percent electrode system for high-resolution EEG and ERP measurements. *Clinical Neurophysiology* 112: 713-719, 2001.

Oscar-Berman M. The effects of dorsolateral-frontal and ventrolateral-orbitofrontal lesions on spatial discrimination learning and delayed response in two modalities. *Neuropsychologia* 13: 237-246, 1975.

Owen A, McMillan K, Laird A, and Bullmore E. N-back working memory paradigm: A meta-analysis of normative functional neuroimaging. *Human Brain Mapping* 25: 46-59, 2005.

Pascual-Marqui R, Esslen M, Kochi K, and Lehmann D. Functional imaging with low-resolution brain electromagnetic tomography (LORETA): a review. *Methods Find Exp Clin Pharmacol* 24 Suppl C: 91-95, 2002.

Passingham R. *The Frontal Lobes and Voluntary Action.* Oxford University Press, 1993.

Pfurtscheller G, and da Silva F. Event-related EEG/MEG synchronization and desynchronization: basic principles. *CLINICAL NEUROPHYSIOLOGY* 110: 1842-1857, 1999.

Picton TW. The P300 wave of the human event-related potential. *J Clin Neurophysiol* 9: 456-479, 1992.

Polich J, and Donchin E. P300 and the word frequency effect. *Electroencephalogr Clin Neurophysiol* 70: 33-45, 1988.

Postle BR. Working memory as an emergent property of the mind and brain. *Neuroscience* 139: 23-38, 2006.

Postle BR, Ferrarelli F, Hamidi M, Feredoes E, Massimini M, Peterson M, Alexander A, and Tononi G. Repetitive transcranial magnetic stimulation dissociates working memory manipulation from retention functions in the prefrontal, but not posterior parietal, cortex. *J Cogn Neurosci* 18: 1712-1722, 2006.

Prager AD, and Contreras-Vidal JL. Adaptation to display rotation and display gain distortions during drawing. *Human Movement Science* 22: 173-187, 2003.

Priebe NJ, Lisberger SG, and Movshon JA. Tuning for spatiotemporal frequency and speed in directionally selective neurons of macaque striate cortex. *Journal of Neuroscience* 26: 2941-2950, 2006.

Prodoehl J, Corcos D, and Vaillancourt D. Basal ganglia mechanisms underlying precision grip force control. *Neurosci Biobehav Rev* 33: 900-908, 2009.

Rizzolatti G, Scandolara C, Matelli M, and Gentilucci M. Afferent properties of periarculate neurons in macaque monkeys. II. Visual responses. *Behav Brain Res* 2: 147-163, 1981.

Roitman AV, Pasalar S, and Ebner TJ. Single trial coupling of Purkinje cell activity to speed and error signals during circular manual tracking. *Experimental Brain Research* 192: 241-251, 2009.

Rosenbluth D, and Allman JM. The effect of gaze angle and fixation distance on the responses of neurons in V1, V2, and V4. *Neuron* 33: 143-149, 2002.

Rosenkilde CE, Bauer RH, and Fuster JM. Single cell activity in ventral prefrontal cortex of behaving monkeys. *Brain Res* 209: 375-394, 1981.

Ruchkin DS, Johnson R, Grafman J, Canoune H, and Ritter W. Distinctions and similarities among working memory processes: an event-related potential study. *Brain Res Cogn Brain Res* 1: 53-66, 1992.

Sauseng P, Klimesch W, Gruber W, Doppelmayr M, Stadler W, and Schabus M. The interplay between theta and alpha oscillations in the human electroencephalogram reflects the transfer of information between memory systems. *Neurosci Lett* 324: 121-124, 2002.

Seidler R, Bloomberg J, and Stelmach G. Context-dependent arm pointing adaptation. *Behavioural Brain Research* 119: 155-166, 2001a.

Seidler RD, Bloomberg JJ, and Stelmach GE. Context-dependent arm pointing adaptation. *Behavioural Brain Research* 119: 155-166, 2001b.

Selemon LD, and Goldman-Rakic PS. Common cortical and subcortical targets of the dorsolateral prefrontal and posterior parietal cortices in the rhesus monkey: evidence for a distributed neural network subserving spatially guided behavior. *J Neurosci* 8: 4049-4068, 1988.

Shah A, Bressler S, Knuth K, Ding M, Mehta A, Ulbert I, and Schroeder C. Neural dynamics and the fundamental mechanisms of event-related brain potentials. *Cereb Cortex* 14: 476-483, 2004.

Slifkin A, Vaillancourt D, and Newell K. Intermittency in the control of continuous force production. *J Neurophysiol* 84: 1708-1718, 2000.

Sosnoff JJ, and Newell KM. Information processing limitations with aging in the visual scaling of isometric force. *Experimental Brain Research* 170: 423-432, 2006.

Srinivasan R, Nunez P, and Silberstein R. Spatial filtering and neocortical dynamics: Estimates of EEG coherence. *Ieee Transactions on Biomedical Engineering* 45: 814-826, 1998.

Stephens JA, and Taylor A. The effect of visual feedback on physiological muscle tremor. *Electroencephalogr Clin Neurophysiol* 36: 457-464, 1974.

Tomita H, Ohbayashi M, Nakahara K, Hasegawa I, and Miyashita Y. Top-down signal from prefrontal cortex in executive control of memory retrieval. *Nature* 401: 699-703, 1999.

Tunik E, Frey SH, and Grafton ST. Virtual lesions of the anterior intraparietal area disrupt goal-dependent on-line adjustments of grasp. *Nat Neurosci* 8: 505-511, 2005.

- Turner RS, Desmurget M, Grethe J, Crutcher MD, and Grafton ST.** Motor subcircuits mediating the control of movement extent and speed. *Journal of Neurophysiology* 90: 3958-3966, 2003.
- Ungerleider LG, and Haxby JV.** 'What' and 'where' in the human brain. *Curr Opin Neurobiol* 4: 157-165, 1994.
- Ungerleider LG, and Mishkin M.** *Two cortical visual systems.* In: Ingle, D.J., Goodale, M.A., Mansfield, R.J.W. (Eds.). Cambridge, MA: MIT Press, 1982.
- Vaillancourt D, Haibach P, and Newell K.** Visual angle is the critical variable mediating gain-related effects in manual control. *Exp Brain Res* 173: 742-750, 2006a.
- Vaillancourt D, Mayka M, and Corcos D.** Intermittent visuomotor processing in the human cerebellum, parietal cortex, and premotor cortex. *J Neurophysiol* 95: 922-931, 2006b.
- Vaillancourt D, and Russell D.** Temporal capacity of short-term visuomotor memory in continuous force production. *Exp Brain Res* 145: 275-285, 2002.
- Vaillancourt DE, Thulborn KR, and Corcos DM.** Neural basis for the processes that underlie visually guided and internally guided force control in humans. *Journal of Neurophysiology* 90: 3330-3340, 2003.
- Vaughan H, Jr.** The relationship of brain activity to scalp recordings of event-related potentials. *Psychophysiology* 13: 54-57, 1969.
- Wager TD, and Smith EE.** Neuroimaging studies of working memory: a meta-analysis. *Cogn Affect Behav Neurosci* 3: 255-274, 2003.
- Wise SP, Boussaoud D, Johnson PB, and Caminiti R.** Premotor and parietal cortex: corticocortical connectivity and combinatorial computations. *Annu Rev Neurosci* 20: 25-42, 1997.
- Woodworth R.** The accuracy of voluntary movement. *Psychological Review-Monograph Supplements* 3: 1899.

APPENDIX

UNIVERSITY OF ILLINOIS AT CHICAGO

Office for the Protection of Research Subjects (OPRS)
Office of the Vice Chancellor for Research (MC 672)
203 Administrative Office Building
1737 West Polk Street
Chicago, Illinois 60612-7227

Approval Notice Continuing Review

June 18, 2010

David Vaillancourt, PhD
Department of Kinesiology and Nutrition
808 S. Wood, AHSB 690
M/C 994
Chicago, IL 60612
Phone: (312) 355-2058 / Fax: (312) 355-2305

**RE: Protocol # 2001-0470
"Functional MR Imaging of Motor Control"**

Dear Dr. Vaillancourt:

Your Continuing Review was reviewed and approved by the Convened review process on June 16, 2010. You may now continue your research.

Please note the following information about your approved research protocol:

Protocol Approval Period: June 16, 2010 - June 15, 2011
Approved Subject Enrollment #: 600 (290 enrolled to date)
Additional Determinations for Research Involving Minors: These determinations have not been made for this study since it has not been approved for enrollment of minors.
Performance Sites: UIC, Northwestern University
Sponsor: 1) NIH - National Institute of Health, 2) NINDS - National Institute of Neurological Disorders and Stroke, 3) NIMH - National Institute of Mental Health, 4) National Institutes of Health, 5) Michael J. Fox Foundation for Parkinson's Research, 6) The Michael J. Fox Foundation for Parkinson's Research
PAF#: 1) 2005-02035, 2) 2008-02184, 3) 2008-05122, 4) 2009-02037, 5) 2001-00795, 6) 2010-01104
Grant/Contract No: 1) R01-NS-52318, 2) R01NS058487, 3) F32 MH083424, 4) R01 NS052318-05A1, 5) Not available, 6) Not available
Grant/Contract Title: 1) Scaling and Sequencing Motor Output in Humans: An fMRI Study, 2) Role of Cortex and Cerebellum in Visually-Guided Motor Behavior, 3) fMRI Studies of Emotion and Movement, 4) Scaling and Sequencing

Phone: 312-996-1711

<http://www.uic.edu/depts/ovcr/oprs/>

FAX: 312-413-2929

APPENDIX (continued)

Page 2 of 4

Motor Output in Humans: An fMRI Study, 5) High Resolution Diffusion Tensor Imaging in Parkinson's Disease and Parkinson Plus Syndromes, 6) Relationship Between REM Behavior Disorder and Freezing of Gait in Parkinson's Disease

Research Protocol(s):

- a) Functional MR Imaging of Motor Control, Version #4, 02/26/2010
- b) Scaling and Sequencing Motor Output in Humans: An fMRI Study; Grant Application dated 9/28/04
- c) NIH grant intitled, "fMRI Studies of Emotion and Movement," as submitted to OPRS on August 21, 2008

Recruitment Material(s):

- a) Motor Control - Statement of Interest, Version 2, 05/13/2005
- b) In Class Announcement Script, Version 3, 10/4/2006
- c) Phone Screen, Version 3, [10/4/2006]
- d) Flyer: "Volunteers Needed 18-35 year olds", V1 10/4/06
- e) Flyer: "Volunteers Needed 36-59 year olds", V1 10/4/06
- f) Flyer: "Volunteers Needed 60-90 year olds", V1 10/4/06
- g) UIC Announce and UIC Massmail Wording 18-35 yrs old, V1 10/4/06
- h) UIC Announce and UIC Massmail Wording 36-59 yrs old, V1 10/4/06
- i) UIC Announce and UIC Massmail Wording 60-90 yrs old, V1 10/4/06
- j) (Form Letter), Version #1, 9/3/2009
- k) Flyer: "Volunteers Needed (Parkinson's Disease)", V2, 04/14/10
- l) Flyer: "Volunteers Needed (Rapid Eye Movement Behavior Disorder)", V2, 04/14/10
- m) Flyer: "Volunteers Needed (Essential Tremor)", V2, 04/14/10
- n) Flyer: "Volunteers Needed (Progressive Supranuclear Palsy)", V2, 04/14/10
- o) Flyer: "Volunteers Needed (Multiple System Atrophy)", V2, 04/14/10
- p) Flyer: "Volunteers Needed (Corticobasal Degeneration)", V2, 04/14/10
- q) Flyer: "Volunteers Needed (Dystonia)", V2, 04/14/10

Informed Consent(s):

- a) UIC Adult Consent: FMRI of Motor Control, Version 20, [3/24/10]

HIPAA Authorization(s):

- a) UIC "Functional MRI Imaging of Motor Control #2001-0470 - Authorization", Version # 2.2, 5/13/2005 (Please continue to use the currently approved Authorization form, approved and stamped June 7, 2005.)

Please note the Review History of this submission:

Receipt Date	Submission Type	Review Process	Review Date	Review Action
05/26/2010	Continuing Review	Convended	06/16/2010	Approved

APPENDIX (continued)

Page 3 of 4

Please remember to:

→ Use your **research protocol number** (2001-0470) on any documents or correspondence with the IRB concerning your research protocol.

→ Review and comply with all requirements on the enclosure,
"UIC Investigator Responsibilities, Protection of Human Research Subjects"

Please note that the UIC IRB has the prerogative and authority to ask further questions, seek additional information, require further modifications, or monitor the conduct of your research and the consent process.

Please be aware that if the scope of work in the grant/project changes, the protocol must be amended and approved by the UIC IRB before the initiation of the change.

We wish you the best as you conduct your research. If you have any questions or need further help, please contact OPRS at (312) 996-1711 or me at (312) 413-7323. Please send any correspondence about this protocol to OPRS at 203 AOB, M/C 672.

Sincerely,



Jennifer Joaquin, MPH
IRB Coordinator, IRB # 1
Office for the Protection of Research Subjects

Enclosure(s):

- 1. UIC Investigator Responsibilities, Protection of Human Research Subjects**
- 2. Informed Consent Document(s):**
 - a) UIC Adult Consent: FMRI of Motor Control, Version 20, [3/24/10]
- 3. Recruiting Material(s):**
 - a) Motor Control - Statement of Interest, Version 2, 05/13/2005
 - b) In Class Announcement Script, Version 3, 10/4/2006
 - c) Phone Screen, Version 3, [10/4/2006]
 - d) Flyer: "Volunteers Needed 18-35 year olds", V1 10/4/06
 - e) Flyer: "Volunteers Needed 36-59 year olds", V1 10/4/06
 - f) Flyer: "Volunteers Needed 60-90 year olds", V1 10/4/06
 - g) UIC Announce and UIC Massmail Wording 18-35 yrs old, V1 10/4/06
 - h) UIC Announce and UIC Massmail Wording 36-59 yrs old, V1 10/4/06
 - i) UIC Announce and UIC Massmail Wording 60-90 yrs old, V1 10/4/06
 - j) (Form Letter), Version #1, 9/3/2009
 - k) Flyer: "Volunteers Needed (Parkinson's Disease)", V2, 04/14/10
 - l) Flyer: "Volunteers Needed (Rapid Eye Movement Behavior Disorder)", V2, 04/14/10
 - m) Flyer: "Volunteers Needed (Essential Tremor)", V2, 04/14/10
 - n) Flyer: "Volunteers Needed (Progressive Supranuclear Palsy)", V2, 04/14/10

APPENDIX (continued)

Page 4 of 4

- o) Flyer: "Volunteers Needed (Multiple System Atrophy)", V2, 04/14/10
- p) Flyer: "Volunteers Needed (Corticobasal Degeneration)", V2, 04/14/10
- q) Flyer: "Volunteers Needed (Dystonia)", V2, 04/14/10

4. Optional Form 310 - Protection of Human Subjects, Assurance Identification/Certification/Declaration

cc: Charles B. Walter, Department of Kinesiology and Nutrition, M/C 517
OVCR Administration, M/C 672

VITA

NAME

Cynthia Poon

EDUCATION

Ph.D., Kinesiology
University of Illinois at Chicago
Chicago, IL, 2012

M.S., Kinesiology
University of Illinois at Chicago
Chicago, IL, 2009

B.S., Kinesiology
University of Illinois at Chicago
Chicago, IL, 2007

HONORS & AWARDS

2011 Movement Disorder Society Travel Grant

2010 UIC Graduate College Student Presenter
Award, University of Illinois at Chicago, Chicago,
IL

2010 UIC Graduate Student Council (GSC) Travel
Award, University of Illinois at Chicago, Chicago,
IL

2010 John E. and Marguerite B. Corbally Award,
University of Illinois at Chicago, Chicago, IL

2007 Cum Laude, University of Illinois at Chicago,
Chicago, IL

2006 & 2007 W.E. Van Doren Scholarship,
University of Illinois at Chicago, Chicago, IL

2006 Helen Barton Summer Research Scholarship
Award, University of Illinois at Chicago, Chicago,
IL

2005-2007 Dean's List of Academic Distinction,
University of Illinois at Chicago, Chicago, IL

VITA (continued)

2003-2004 Merit Recognition Scholar, University of Illinois at Chicago, Chicago, IL

PROFESSIONAL & TEACHING EXPERIENCE

2009-Present, Graduate Research Assistant, Neural Control of Movement Laboratory, Department of Kinesiology and Nutrition, University of Illinois at Chicago, Chicago, IL

2007-2009, Graduate Teaching Assistant
Department of Kinesiology and Nutrition,
University of Illinois at Chicago, Chicago, IL

2006-2007, Undergraduate Research Lab Assistant, Neural Control of Movement Laboratory, Department of Kinesiology and Nutrition, University of Illinois at Chicago, Chicago, IL

SOCIETY MEMBERSHIPS

2011-Present, Member
Movement Disorders Society

2009-Present, Member
Society for Neuroscience

2007-2009, Member
Society for Neural Control of Movement

PUBLICATIONS

Poon C, Robichaud J, Corcos DM, Goldman JG, Vaillancourt DE. Combined measures of movement and force variability distinguish Parkinson's disease from essential tremor. *Clinical Neurophysiology*. 2011. 122: 2268-2275.

Shapiro MB, Niu CM, **Poon C**, David FJ, Corcos DM. Proprioceptive feedback during point-to-point arm movements is tuned to the expected dynamics of the task. *Experimental Brain Research*. 2009. 195: 575-591.

David FJ, **Poon C**, Niu CM, Corcos DM, Shapiro MB. EMG responses to unexpected perturbations

VITA (continued)

are delayed in slower movements. *Experimental Brain Research*. 2009. 199(1): 27-38.

PUBLICATIONS IN PROGRESS

Poon C, Chin-Cottongim L, Coombes S, Corcos DM, Vaillancourt DE. Spatiotemporal evolution of brain activity during the transition from visually guided to memory guided force control. *Journal of Neurophysiology*. 2012.

Poon C, Coombes S, Corcos DM, Christou E, Vaillancourt DE. Adaptations to enhanced visual information cause transient shifts in brain activity in parietal-frontal circuits that relate to motor performance. *Neuroimage*. 2012.

Corcos D, Robichaud J, David F, Vaillancourt D, **Poon C**, Rafferty M, Comella C, Kohrt W, Leugans S. A two-year randomized clinical trial of progressive resistive exercise in Parkinson's disease. *Journal of the American Medical Association* 2012.

CONFERENCE PRESENTATIONS

Poon C, Robichaud J, Corcos DM, Goldman JG, Vaillancourt DE. Combined measures of movement and force variability distinguish subjects with Parkinson's disease (PD) from Essential tremor (ET). *International Congress of Parkinson's Disease and Movement Disorders at Toronto, Canada, 2011.*

Poon C, Chin-Cottongim L, Coombes S, Corcos DM, Vaillancourt DE. Spatiotemporal dynamics during the transition from a visually guided to a memory guided force control task: an EEG-ERP study. *Society for Neuroscience, San Diego, CA, 2010.*

Vaillancourt, D.E. and **Poon, C.** Movement and brain function abnormalities in Essential tremor and Parkinson's Disease. *International Congress of Clinical Neurophysiology, Kobe, Japan, 2010.*

VITA (continued)

Niu CM, **Poon C**, David FJ, Corcos DM, Shapiro MB. Proprioceptive feedback during movement is facilitated at the time of expected peak in joint torque. Society for the Neural Control of Movement. Naples, Florida, 2008.

David FJ, **Poon C**, Niu CM, Corcos DM, Shapiro MB. EMG responses to unexpected perturbations are delayed in slower movements. Society for the Neural Control of Movement. Naples, Florida, 2008.

Poon C, Shapiro M, David FJ, Niu CM, Corcos DM. Activity of proprioceptive feedback pathways during point-to-point movements. Undergraduate Research Symposium at the University of Illinois at Chicago, 2007.